Summer 2007

# Fine particle classification using dilute fluidized beds

Rajasekharan Pillai Annapoorneswari



Department:

# FINE PARTICLE CLASSIFICATION USING DILUTE FLUIDIZED BEDS

By

RAJASEKHARAN PILLAI ANNAPOORNESWARI

A THESIS

Presented to the Faculty of the Graduate School of the

UNIVERSITY OF MISSOURI-ROLLA

In Partial Fulfillment of the Requirements for the Degree

MASTER OF SCIENCE IN CHEMICAL ENGINEERING

2007

Approved by

| | |
|---|---|
| _____ | _____ |
| Dr. Kimberly Henthorn, Advisor | Dr. Douglas Ludlow |

_____

Dr. Delbert Day

# ABSTRACT

Fluidized beds have been used for a variety of industrial applications. The aim of this project is to narrow the size distribution of a particle sample using a dilute continuous fluidized bed. The particles were separated based on their settling velocities, and the effects of various parameters were studied. In a jacketed column, the upward water velocity was adjusted so that glass particles larger than the desired size settled to the bottom, while smaller particles were carried upward. The separation efficiency was increased by adding inclined reflux plates. This process was found to be a better method to classify small particles, than the other methods of classification. Since the current research involves small particles, this particular process was chosen. In addition, the cohesive nature of these small particles eliminates the feasibility of effectively classifying particles using a dry separation process such as sieving. Within the ranges studied, the particle feed rate, plate angle, number of plates, and column shape did not show any significant effect on the classification of particles. The most critical criterion for particle classification was found to be the water flow rate. However, particle classification based on plate length showed an increasing trend with respect to an increase in plate length. The particle size distributions for the overflow (top fraction) and underflow (bottom fraction) were slightly underpredicted theoretically when compared to the experimental particle size distributions obtained.

# ACKNOWLEDGMENTS

First and foremost, I would like to thank my advisor, Dr. Kimberly Henthorn, for her guidance and supervision throughout my curriculum at the University of Missouri–Rolla. Without her guidance it would have been impossible for me to reach this point. She was my guiding light and I would be totally lost without her. I have heartfelt gratitude towards her, and it is difficult to encompass the respect and affection I have for her in words. I would like to thank Mo-Sci and Dr. Delbert Day, without whom the project would have never materialized. I would like to thank Dr. Douglas Ludlow for his assistance as a committee member, as well as professors Dr. David Henthorn, Dr. Neil Book, Dr. A. I. Liapis, and Dr. Judy Raper and Dr. Yangchuan Xing for their valuable time and willingness to help me. Also, my thanks go to Dean Lenz, our lab technician, whose support was invaluable for the project. I wish to thank all the staff members of the Chemical Engineering Department of the University of Missouri–Rolla, but especially Audrey Morris (AJ), Tealok Ray and Marlene Albrecht, who gave me terrific help in a lot of administrative and logistic aspects.

Without my family I would be nowhere, so I would like to thank my family for always being there for me. I would like to thank my good friends Anish, Shanti, Navina, Sumesh, Mihir and Soumya for offering me all the mental and emotional support I need. They are like my second family, and without them it would be very difficult for me to accomplish this. In addition, I would like to thank all my other friends who have been there for me in times of need.

# TABLE OF CONTENTS

Page

# LIST OF ILLUSTRATIONS

# 1. INTRODUCTION

The need for particle classification processes has existed for many decades. Particle classification is important as there are various applications that require narrow size distributions, including those in the medical, pharmaceutical, drug delivery, consumer product, microchip, and automotive industries. As particle size decreases, particle-particle interactions and interparticle forces increase and it becomes very difficult to classify them by sieving or other dry classification methods. As a result, hydroseparation processes are found to work best for very small or cohesive materials. One of the oldest and most commonly used wet classification methods is based on gravitational settling. Settling is the process by which particles move down under the influence of a force, which is typically a gravitational or centrifugal force, and accumulate at the bottom of a vessel. Numerous separation techniques exist, but the physical reason behind particle separation and methods of improving efficiency of separation in fluidized beds will be investigated here. Fluidized beds are used for a number of operations including coal combustion, promotion of reactions, and classification of particles. The very dilute fluidized beds used here are considered to be hydro-separators, where the particles are separated based on their settling velocities.

## 1.1. MOTIVATION

Size classification of small particles has always been tedious due to their cohesive nature, and since recent thrusts have focused on small scale applications, classification of small particles has become crucial, especially in pharmaceutical and biological fields. Many applications require the use of extremely narrow particle size distributions, such as particle-based cancer treatments, drug delivery, MRIs, blood flow studies, commercial spacers, and frictionless coatings (Mo-Sci. Corp., Rolla, MO)[1,2,3,4,5]. For example, one particle-based cancer treatment utilizes injected radioactive glass particles which target the cancerous region without physically migrating throughout the tissue. In some controlled-release drug delivery applications, the active drug is placed inside the glass particles and slowly diffuses out once inside the body. Similarly, in MRI and blood flow studies, magnetic and fluorescent glass particles facilitate visualization of the fluid flow.

Glass microspheres are used in gas plasma displays, electronic displays, flip chip technology, filters, sporting goods equipment, calibration standards, and transformer manufacturing (Mo-Sci. Corp., Rolla, MO).

Glass spheres can also be used as spacers in the manufacturing of automotive rearview mirrors to obtain an accurate micro-scale separation between the reflective surface and the protective glass. It is essential to have a narrow particle size distribution to achieve uniform spacing throughout the sample. Figure 1.1 illustrates the how these systems work. Research to integrate hollow glass spheres into the manufacture of plasma

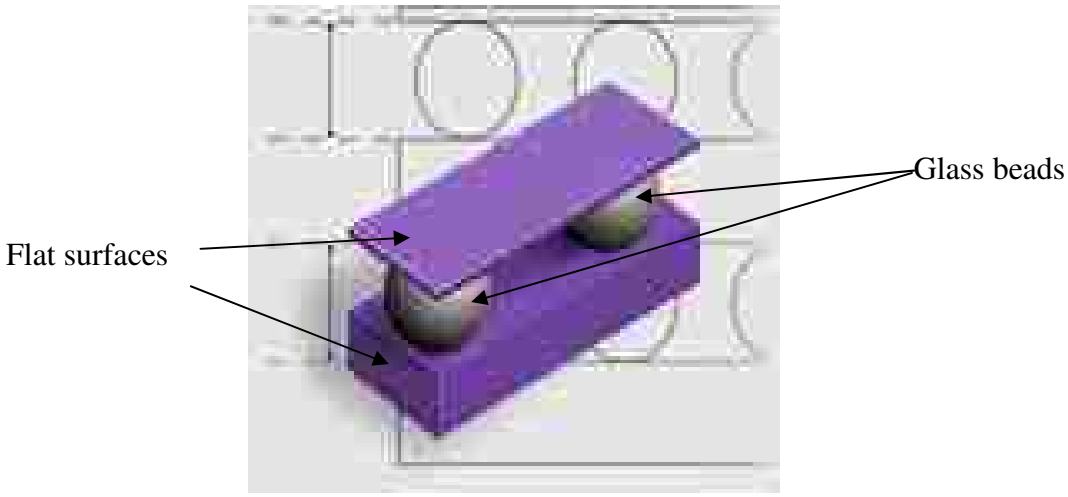


Figure 1.1 Use of Glass Spheres as Spacers[6]

screens is currently being pursued by Grinspon et al.[7] The hollow glass spheres hold ionizable gas (plasma), and the innate strength of the hollow glass spheres makes the plasma displays more rugged. In conventional plasma displays, two glass substrates are sealed to each other air tight, making them very heavy. The new design is much more lightweight and affordable because expensive technology is not required to create an air tight seal. If the spheres have a wide distribution, the surface will become distorted and the quality of the display will be poor, so it is important that the spheres are monodisperse. Glass beads can also be used to coat optical fibers to reduce the friction

between the optical fiber and the sheath, and can be formed into scratch resistant films for automobiles and cooking utensils[8]. In all these applications, precise particle size is critical for the process to work and requires that the particles are accurately separated to extremely narrow particle size distributions.

## 1.2. OBJECTIVES

The main objective of this project is to classify spherical soda-lime glass particles based on their size using a dilute fluidized bed system. The influence of inclined plates in the column, plate separation, plate inclination, and number of plates on the overall separation efficiency of particles will be investigated. The effect of column shape on the classification efficiency will also be assessed.

## 1.3. BACKGROUND

**1.3.1. Types of Classification Processes.** Classification, sometimes called grading, is the general term given to the operation of separating solid particles and is carried out by splitting a mixture into two or more fractions. Each fraction will be more homogeneous in size than the original mixture. Solids can be classified based on various properties, including size, shape, specific gravity, surface roughness, color, and magnetic properties. The differences in any of these properties can be exploited to classify the particles. Although there are many techniques of classification, the most common methods of classification are based on particle size, particle shape, and the specific gravity of the particle; this is schematically represented in Figure 1.2.

Classification processes can also be divided into two major types based on the medium of suspension: wet classification and dry classification. Particles are suspended in a liquid during wet classification processes. By suspending the particles in a liquid phase, the interparticle forces are reduced. Some methods can be classified as either wet or dry methods and are only different in the way the equipment is operated. Popular classification methods include cyclone separation, electrostatic precipitation (ESP), filtration, and sieving, each of which is detailed below.

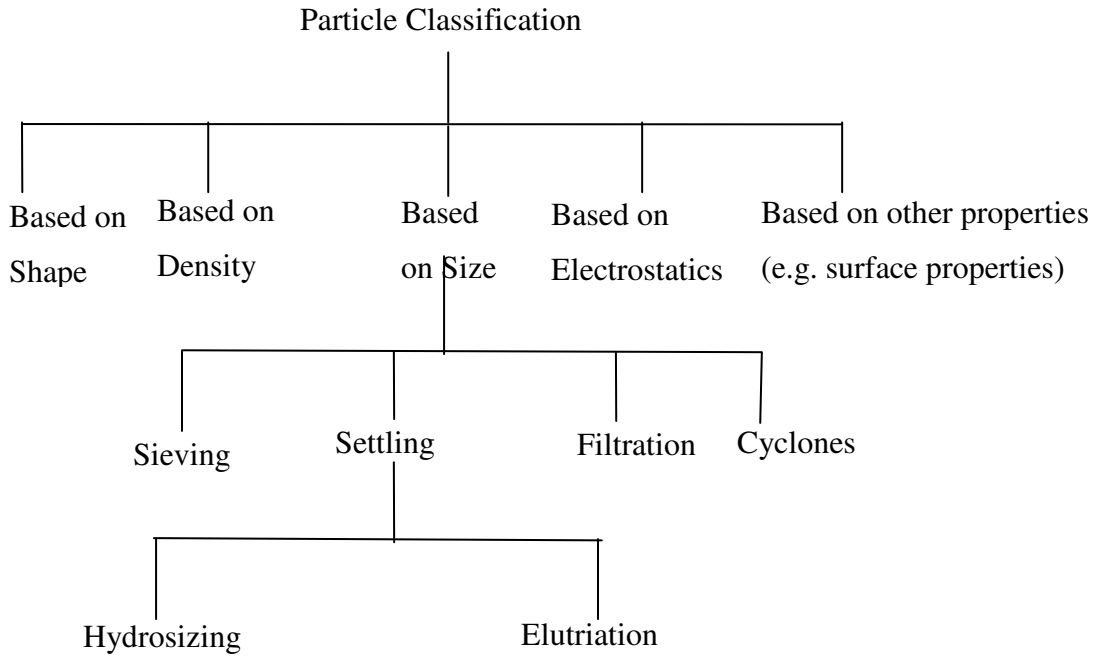


Figure 1.2 Various Methods of Classification[9]

**1.3.1.1. Cyclone separation.** Cyclone separators can be operated as either dry or wet classifiers; cyclones treating particles suspended in water are called hydrocyclones. Hydrocyclones were designed and patented in 1891 by Bretney[10] to suppress the effect of interparticle forces at reduced particle sizes. Hydrocyclones are used in industry for liquid clarification, slurry thickening, degasification of liquids, classification of solids, and two-phase separation[10].

The operating principle for both hydrocyclones and gas-phase cyclones is the same. In both methods, the feed is sent tangentially into the cyclone and the particles swirl down the conical portion of the body (Figure 1.3)[11]. A vortex is created due to spin created by the shape of the cone. Heavier particles are forced outward to the walls of the cyclone where the drag of the spinning fluid and the force of gravity cause them to fall down the sides of the cone into the outlet at the bottom[10, 11]. Lighter particles, along with the gas or liquid medium, exit through the top of the cyclone through the low pressure center. Effective cyclone operation requires a steady flow, free of fluctuations or short term variations in the flow rate. Cyclone separators are 50-75% efficient and have low

maintenance costs. However, particles may tend to break due to attrition and shear, and may also aggregate or agglomerate due to interparticle forces between small particles, which could lead to a poor classification.

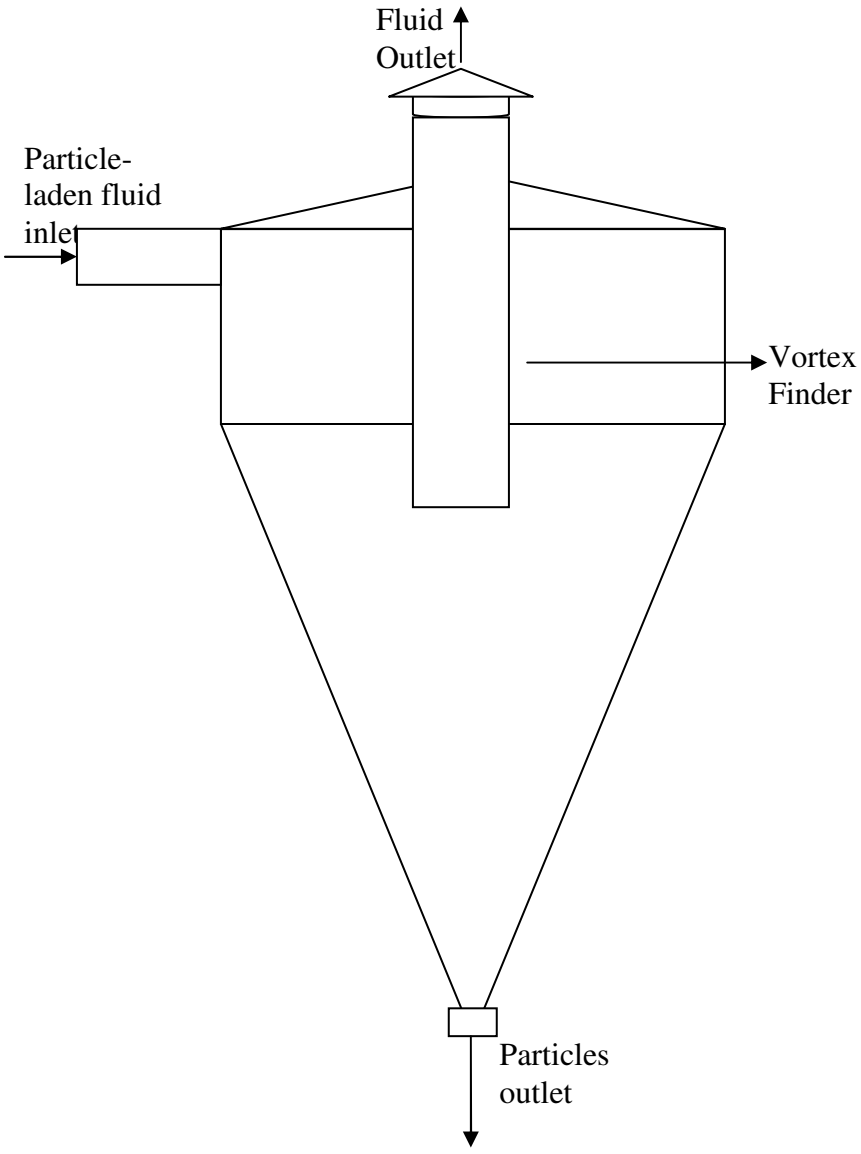


Figure 1.3 Schematic Diagram of a Cyclone

**1.3.1.2. Electrostatic precipitation.** Electrostatic precipitators (ESPs) are used to separate very fine particles from a gaseous stream and can be operated under either wet

or dry conditions. In wet ESPs, the incoming particle-laden gas is sprayed with moisture to remove the extremely fine particles that cause electrical resistance. The gas-particle mixture passes through an electric field created by a discharge electrode, where the particles obtain a negative charge. The particles are attracted to a collection electrode, which is positively charged or grounded, and are collected on the collection electrode and removed. Figure 1.4 is a schematic diagram showing the operating principle of ESPs and Figure 1.5 shows the typical layout of an industrial ESP.

ESPs have low operating costs and low energy requirements because they work only on the particulate matter and do not obstruct the flow. Although ESPs operate with low pressure drops, they have relatively high capital costs. The wire discharge electrodes require high maintenance due to corrosion; however, recent designs include rigid electrodes that are more resistant to corrosion[12]. ESPs can only separate particles smaller than 5 microns because larger particles cannot be charged to saturation as easily as the smaller ones.

**1.3.1.3. Filtration.** Filtration is one of the most common methods for particle separation and is widely used in the treatment of wastewater. This type of separation process is driven by the interaction and pressure difference of a solid-liquid mixture across filter media. Pressure filters, vacuum filters, and centrifugal filters are most commonly used for industrial applications. Common filter media include filter paper, diatomaceous earth, expanded perlite, sintered glass, mesh, sand, and fabric[13].

There are three main types of filters: cake filters, clarifying filters, and cross-flow filters. Plate and frame filter presses, rotary vacuum filters, centrifugal filters and bag filters are examples of cake filters, which separate very large amounts of solids from a solid-liquid mixture as a cake (suspended particles retained on the filter media). Centrifugal filters are a type of cake filters and they are used to filter out solids that form a porous cake. The feed is sent into a rotating basket with perforations and the solids separate out under the influence of centrifugal force. Clarifying filters remove small quantities of solids from a gas-solid mixture or a solid-liquid mixture by trapping it on or inside the filter medium. There is no noticeable cake formation in a clarifying filter as the concentration of solids is very low. In cross-flow filters, the solid-liquid mixture is passed over a porous surface and due to differential pressure, some of the liquid passes

through the membrane and is collected as filtrate and the rest of the liquid is recycled through the system[13].

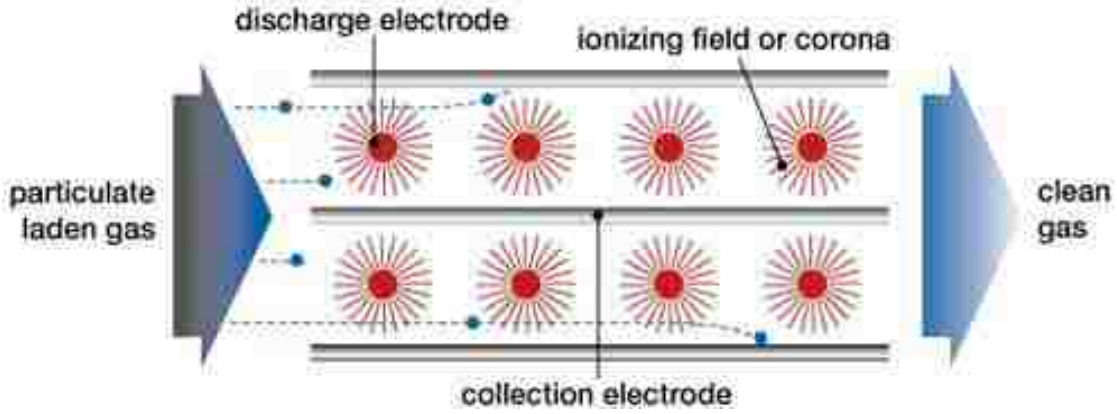


Figure 1.4 Schematic Diagram of ESP[14]

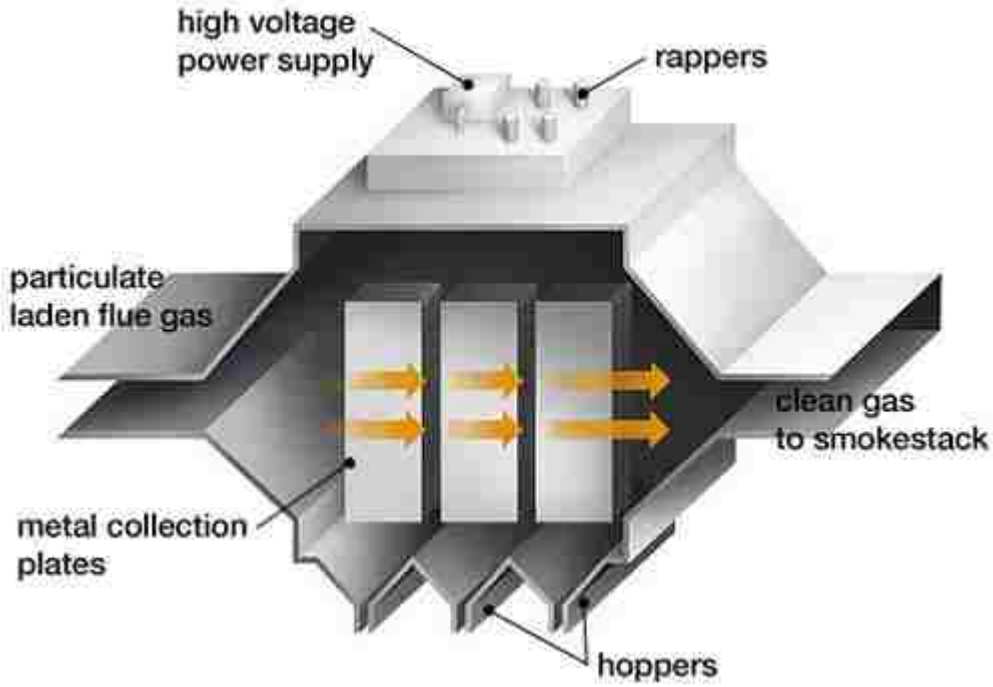


Figure 1.5 Schematic Diagram of an Industrial ESP[14]

**1.3.1.4. Sieving.** Sieving is a method of particle classification where the passage of particles is limited or controlled by a mechanical screen. A series of screens with decreasing diameter openings is used to classify particles into various size ranges. The

particles are agitated on top of a cloth screen or mesh and particles that are smaller than the opening of the mesh or screen fall through due to the force of gravity. Only particles larger than 45 microns can be separated by sieving, because interparticle forces promote aggregation between very small particles, which makes sieving difficult. Sieving is typically a dry separation method, but wet sieving can also be done to reduce interparticle forces and classify particles as small as 5 microns in size.

Sieving is the cheapest and most uncomplicated method of separation but it has a few disadvantages. Sieving is not reliable for highly non-spherical particles, such as needle-like particles, because particle orientation and mobility is important in order to pass through the sieve openings. In addition, aggregation or agglomeration of particles is a major disadvantage even while using wet sieving, and electrostatic forces are prominent in dry sieving because of triboelectrification, or charging due to rubbing[15].

**1.3.2. Hydrosizing.** Hydrosizing is strictly a wet method and hydraulically separates particles based on their settling velocities. A particulate slurry is fed into an upward-flowing liquid stream and the particles are separated based on their terminal settling velocity; particles with a higher settling velocity than the liquid velocity settle downward and those with a smaller terminal settling velocity are carried upward with the liquid. The principle of such separation is the viscous drag dependency on particle size, shape or density. Hydrosizing gives the least aggregation and least breakage compared to a cyclone separators, and can be run as a continuous process.

The settling of particles in shallow beds for wastewater treatment was studied first by Hazen in 1904 and was further explored by Camp in 1946[16]. In 1851, Stokes derived an equation for the viscous resistance to the motion of a single spherical particle in an infinite fluid, which is now known as the Stokes equation. From 1942, fluidization techniques were used for the catalytic cracking of high boiling petroleum fractions. One of the most referred publications in fluidization and sedimentation is the work of Richardson and Zaki in 1954[17]. They studied multi-particle settling and fluidization and developed equations for bed porosity and other relationships that are widely used today. They also found that for vertical hydraulic transport the liquid velocity should exceed the terminal settling velocity of the particle, and that at low concentrations of particles, wall effects were more prominent. Fluidization has historically been effective in particle

separation, but typically in dense phase operation. Fluidization has recently been used by Rasul et al. to separate and classify cohesive mineral particles[18].

Reflux classifiers (developed by Galvin and Nguyentranlam in 2000) couple fluidization with the operating principle of lamella separators (sedimentation tanks with inclined parallel plates), and are used in industry for various particle classification needs[19]. Fluid containing the suspended solids flows through channels created by parallel plates in the column, and some particles with terminal settling velocities near the liquid velocity separate and settle onto the plates. It is this segregation action of the plates that allow for better classification. The plates cause a reflux action, which is a consequence of the settling of the fluidized particles onto the inclined plates and returning to the fluidized zone below. These settled particles then slide down into the fluidized zone where small particles with lower settling velocities are re-entrained, increasing the overall separation efficiency. In fluidized beds containing inclined parallel plates, it is possible to obtain a wide range of suspension concentrations at a single fluidization velocity. Suspensions can be formed at liquid velocities much greater than the particle terminal velocity because of the varied flow rates obtainable within the plates. Galvin and Nguyentranlam found that the presence of plates significantly increased the separation efficiency[20].

Galvin and Nguyentranlam investigated the influence of inclined parallel plates at different heights using the same fluidization rate. They found that the suspension concentration within the fluidized bed increased when the parallel inclined plates were moved closer to the feed point. This agreed with their predicted model, which was based on a single-particle force balance inside the inclined channel. They studied only the effect of plate location in the column, and we have extended their work here by investigating the effects of inclination angle and plate spacing. They conducted experiments in a column a 0.4 m square column, 1.5 m high[19, 20]. This process was done iteratively until all the particles were either settled or carried out through the top of the column.

In general, a fluidized bed works in association with the imposed fluidization superficial velocity (the velocity of the fluid across the column cross-section), $u_o$ and the

resulting volume fraction of solids, $\phi_s$. The Richardson-Zaki equation describes this relationship for a single particle species[17]:

$$u_o = V_s f(\phi_s) \tag{1.1}$$

where $V_s$ is the terminal velocity of a single isolated particle in the liquid.

$$f(\phi_s) = (1 - \phi_s)^n \tag{1.2}$$

where n is the hindered settling factor with n≈ 4.6 at low Reynolds numbers[20].

Galvin and Nguyentranlam found that the suspension concentration increased when the parallel inclined plates were lowered and their experimental results agreed with the predicted theoretical models[20, 21]. The consequences of having an inclination in the bed configuration have been investigated in prior work by various researchers. The "tilted-plate separator" was reported as one of 1969's top ten pieces of equipment in *Chemical Engineering, 1970.* It was reported to have better separation efficiency and occupied only 1/6 of the floor space compared to a separator without plates[22]. The body of the separator was tilted, which seemed to be the reason for the reduction in floor space as compared to having a settling tank. Particles larger than 10 μm were completely removed from wastewater containing a suspension of filter earth, and by having no power requirements and no moving parts, it required less maintenance as well. It was reported that when the direction of flow of the wastewater was in the upward direction the heavier particles dropped out and when the direction of flow was reversed the lighter particles that formed scales on the sides were washed off.

Davis et al. moved away from traditional dense phase fluidization and investigated dilute phase fluidization[23]. Zhang and Davis studied two different experimental setups to classify dilute particle suspensions into a coarse bottom fraction and a fine top fraction[24]. One configuration involved one inclined settler in which some of the coarse fraction was recycled, and the other included two inclined settlers in series where the coarse fraction was not recycled. A number of narrow distributions were obtained by using the second setup. The experimental results obtained from the two

schemes were in good agreement with the theoretical predictions they made based on a material balance on the feed, overflow (fine fraction), and underflow (coarse fraction) streams. They concluded that if an appropriate recycle ratio was used, the inclination of the settler was as large as possible, and the underflow rate was as low as possible, flow instabilities can be avoided and particle classification can be improved. They observed that flow instabilities created by recycling caused some of the resuspended particles to be smaller than the cut-off size and thus they were carried out through overflow rather than being withdrawn from the underflow.

**1.3.3. Types of Settling.** Settling is the process by which the particulate matter in a liquid is removed by allowing the particles to settle under the influence of gravity, and it is classified into four types based on the concentration of particles in the liquid. It is important to classify the type of settling as it helps to better understand the mechanisms of settling. The four major types of settling are classified as Type I, Type II, Type III, and Type IV which are detailed below:

**1.3.3.1. Type I.** Type I settling is characterized by the free settling of particles without the influence of other particles and typically occurs in very dilute suspensions. Particles with a given settling velocity follow a straight trajectory and other particles with the same settling velocity follow parallel trajectories. Particles in Type I settling accelerate with a constant velocity until the drag force becomes equal to the impelling force, after which they travel with a constant velocity called the terminal velocity or the settling velocity. The following equation gives the impelling force, $F_I$:

$$F_I = (\rho_s - \rho)\, g\, V \tag{1.3}$$

where $\rho_s$ is the mass density of the particle, ρ is the mass density of the liquid, V is the volume of the particle, and g is the acceleration due to gravity. The equation for drag force, $F_D$ is given by Newton's Law as:

$$F_D = C_D\, A_c \rho \left(\frac{V_s^2}{2}\right) \tag{1.4}$$

where $C_D$ is the drag coefficient, $A_c$ is the cross-sectional area, and $V_s$ is the settling velocity. When the impelling force becomes equal to the drag force, the settling velocity for a sphere with a diameter, d, is given by the equation given below:

$$V_s = \left[ \frac{4g(\rho_s - \rho)d}{3C_D\rho} \right]^{1/2} \tag{1.5}$$

where the numerical value of $V_s$ changes with the flow regime (turbulent, transitional, or laminar) about the particle because the term $C_D$ in the equation is dependent on the flow regime. The dependence of the settling velocity on flow regime is due to the drag force, which varies with Reynolds number. The relationship between the drag coefficient and the Reynolds number, when the flow is in Stokes regime ($Re_p < 0.1$) is given by:

$$C_D = \frac{24}{Re_p} \tag{1.6}$$

where $Re_p$ is the particle Reynolds number and $\mu$ is the dynamic viscosity of the fluid. The Reynolds number for spheres is given by the following equation:

$$Re_p = \frac{\rho d V_s}{\mu} \tag{1.7}$$

**1.3.3.2. Type II.** Type II settling describes the settling of flocculent particles. In Type II settling the particles are in a dilute concentration, but tend to stick to one another and form flocculents, which settle at a faster rate than in single particle settling. To determine the settling velocities of the flocculent, batch settling tests are used. Batch tests are carried out in quiescent conditions and the temperature is held constant throughout the column to avoid convection. The overflow rate and percent removal can be calculated from these batch tests by measuring the volume of the overflow and determining the weight of the dry solids in it.

**1.3.3.3. Type III.** Type III settling is the known as zone or hindered settling. Type III settling occurs in a comparatively high concentration of particles. Due to the high concentration of the particles, the particles are so close together that the interparticle forces hinder the settling of neighboring particles. The particles settle at a constant velocity so the particles remain in the same position relative to the other particles, which causes the particles to settle in zones. A discrete solid-liquid interface exists above the settling particles.

**1.3.3.4. Type IV.** Type IV settling is known as compression settling, which occurs when the concentration of particles is much higher than is required for Type III settling. In compression settling, the concentration of particles is so high that they touch each other and settling can occur only by compaction of the particles; that is, the particles are pushed downward. The common types of particles to undergo compression settling are flocculent particles, though even discrete particles can settle by compression settling.

# 2. THEORY

The governing equations for particle settling within an inclined channel are presented here. Two approaches have been taken: one based on a single particle settling within the inclined channel, and the other with many particles settling within the channel.

## 2.1. SINGLE PARTICLE SETTLING

The system considered is a single particle in an inclined channel (Figure 2.1). The theoretical analysis discussed in this section is an extension of the work presented by Galvin and Nguyentranlam[19, 20]. In their analysis they considered the particle slip velocity, $u_s$, as the sum of the vertical ($u_{sy}$) and horizontal ($u_{sx}$) components of the particle slip velocity (the velocity difference between the particle and the fluid).

$$u_s = u_{sx} + u_{sy} \tag{2.1}$$

where

$$u_{sx} = u_s \sin\theta \tag{2.2}$$

$$u_{sy} = u_s \cos\theta \tag{2.3}$$

and $\theta$ is the angle of inclination of the plate from the horizontal plane.

The equation developed by Grbavcic and Vukovic gives the slip velocity for a single particle settling in a dilute fluidized bed[25]:

$$u_s = \frac{u_o}{(1-\phi_s)} + V_s \tag{2.4}$$

where $V_s$ represents the settling velocity of a sphere in the Stokes regime and is expressed as

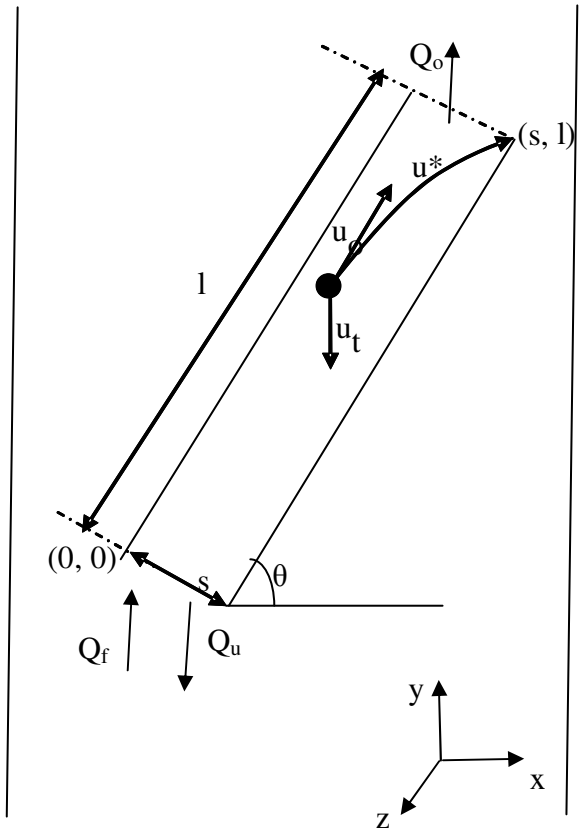


Figure 2.1 Schematic Representation of a Single Set of Inclined Plates in the Column

$$V_s = \frac{(\rho_s - \rho)d^2 g}{18\mu} \tag{2.5}$$

The following equation was developed by Galvin and Nguyentranlam based on a single particle settling in an inclined channel[19,20]:

$$\frac{dy}{dx} = \frac{u_o - u_s(1-\phi_s)\sin\theta}{u_s(1-\phi_s)\cos\theta} \tag{2.6}$$

Equation (2.6) is integrated from location (0, 0) to (s, l) to obtain the critical terminal velocity, $u^*$, of the particle, which is the minimum settling velocity that a particle must have to settle on to the inclined plate (Figure 2.1):

$$u^* = u_s(1-\phi_s)[\sin\theta + \frac{l}{s}\cos\theta] \tag{2.7}$$

where l is the length of the plates and s is the spacing between them.

By assuming Stokes law applies between the plates, Equations (2.5) and (2.7) are equated to obtain the following equation:

$$d_p{}^2 = \frac{18\mu u_s[\sin\theta + \frac{l}{s}\cos\theta]}{g(\rho_p - \rho)} \tag{2.8}$$

Substituting the value of $u_s$ from Equation (2.4) into Equation (2.8) and simplifying, an equation for the cutoff diameter (the diameter of the particle having the critical terminal settling velocity), $d_p$, is obtained:

$$d_p = \sqrt{\frac{18\mu u_o[\sin\theta + \frac{l}{s}\cos\theta]}{g(\rho_p - \rho)[1-(1-\phi_s)(\sin\theta + \frac{l}{s}\cos\theta)]}} \tag{2.9}$$

## 2.2. MULTIPLE PARTICLE SETTLING

Davis et al., first investigated the segregation of particles using inclined channels[26]. The results they obtained experimentally were concurrent with the theory they derived and it was demonstrated again in their future publications [23, 24]. The equation they derived has been modified to be appropriate for the system that was studied in this work and has been briefly explained below.

A sketch of the inclined channel in the column is given in Figure 2.1, and a mass balance on the channel yields the following set of equations.

$$Q_f = Q_u + Q_o \tag{2.10}$$

$$Q_f \phi_f = Q_u \phi_u + Q_o \phi_o \tag{2.11}$$

$$Q_f \phi_f P_f(u) = Q_u \phi_u P_u(u) + Q_o \phi_o P_o(u) \tag{2.12}$$

where $Q_f$, $Q_u$, $Q_o$ are the volumetric flow rates of water fed into column, underflow rate of water, and overflow rate of water, respectively, and $\phi_f$, $\phi_u$, and $\phi_o$ are the solid fractions in the feed, underflow, and overflow, respectively. $P_f(u)$, $P_u(u)$, and $P_o(u)$ are the probability density functions for distributions of particle settling velocities of the feed, underflow, and overflow, respectively. In the experiments carried out in this work, there was no liquid underflow; therefore $\phi_u$ was taken as 1.

It was found by statistical analysis that the feed followed a normal distribution with the probability density function given below:

$$P_f(d) = \frac{1}{\sigma\sqrt{2\pi}} e^{-\left(\frac{(d-\bar{d})}{2\sigma^2}\right)^2} \tag{2.13}$$

where $\bar{d}$ is the mean diameter of the particle feed distribution and $\sigma$ is the standard deviation.

The probability density function based on particle diameter was converted to a probability density function based on particle settling velocity by the relation given by Davis et al[23].

$$P_f(u) = P_f(d)\frac{dd}{du} \tag{2.14}$$

By substituting Stokes law into Equation 2.14 the following equation was derived:

$$P_f(u) = \frac{9\mu P_f(d)}{(\rho_p - \rho_f)gd} \tag{2.15}$$

Davis et al. derived the following equation from Equation 2.15 for the probability density function for the distribution based on particle settling velocities in the overflow:

$$P_o(u) = \frac{(Q_o - S(u))P_f(u)}{\int_0^{v_o} (Q_o - S(u))P_f(u)du} \tag{2.16}$$

where S(u) is the settling velocity of particle between the inclined plates, which is given by:

$$S(u) = V_s w(l\cos\theta + s) \tag{2.17}$$

where w is the width of the inclined plates and the term $w(l\cos\theta + s)$ is the horizontal projected area of the plates. The probability density function for the distribution of settling velocity for the underflow is:

$$P_u(u) = \frac{Q_f P_f(u) - P_o(u)\int_0^{u_o} (Q_o - S(u))P_f(u)du}{Q_f - \int_0^{u_o} (Q_o - S(u))P_f(u)du} \tag{2.18}$$

The probability density functions based on settling velocities for both underflow and overflow are reconverted to diameter-based probability distribution functions using the Stokes equation.

# 3. EXPERIMENTAL PROCEDURE

## 3.1. MATERIALS

The particle injection port was made of steel and the particles used in the experiment were spherical soda lime cobalt glass and soda lime glass particles from Mo-Sci. Corp., Rolla, MO. For initial qualitative experiments, blue soda lime cobalt glass spheres with a size ranging from 4-90 µm and a mean diameter of 30 µm were used. A second sample of glass beads used in the quantitative experiments were colorless soda lime glass spheres, which had a size range of 3-60 µm and a mean diameter of 22 µm. The density of all the glass particles was approximately 2.5 g/cm$^3$. A representative particle size distribution of the soda lime glass spheres is given below in Figure 3.1. The secondary peak seen in the distribution will be discussed in detail later.

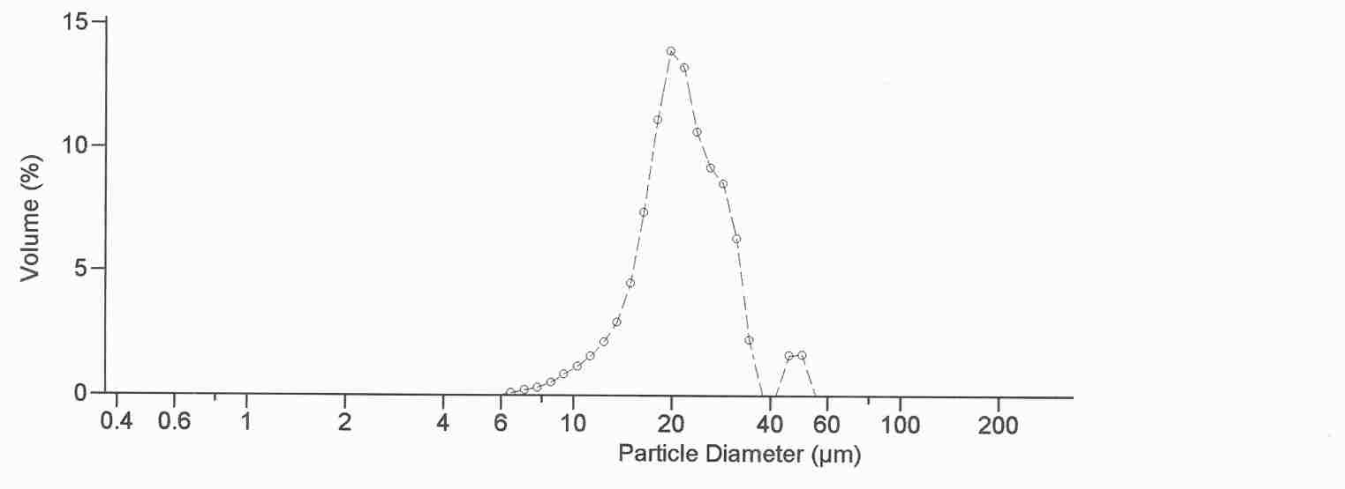


Figure 3.1 Representative Particle Size Distribution of the Feed

## 3.2. WATER AND WATER QUALITY

Bubbles were present on the column walls when the column was initially filled with tap water, and as it was expected that the bubbles would affect the flow profile and the particles would stick to the bubbles and cause undesired segregation, it was necessary

to get rid of them. Upon investigation, it was found that tap water is generally aerated by water treatment plants to improve the taste. To overcome this, tap water was replaced by distilled water for the experiments, which eliminated the problem.

### 3.3. PARTICLE LOADING

Particle injection into the column was initially performed manually using a dropper. Precise feed rates could not be achieved by this manual method, so a rotary peristaltic pump (Masterflex L/S®) was used to feed particles. Feed rates were more precise and more controlled with this method. The particle slurry (~1.6 g/mL) was first injected into the end of Tygon tubing (ID: 0.5 cm, OD: 0.75 cm) that was connected to the particle injection port of the column, while the other end ran through the pump into a beaker filled with water (Figure 3.2). The particle slurry was not fed directly into the peristaltic pump for the fear of glass particles being broken by its rotary action. Particle agglomeration was noticed only when pure particle-water (slurry) was fed into the column. This was easily overcome by adding a drop of Tween 80 surfactant (~2 wt %) to the slurry.

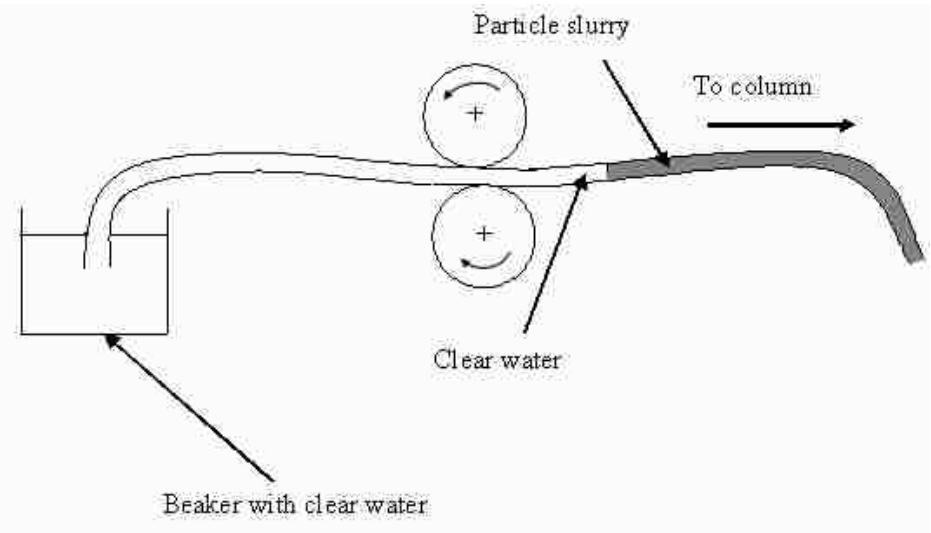


Figure 3.2 Sketch of Peristaltic Pump Loading Particles

### 3.4. EXPERIMENTAL SETUP

The experimental setup consisted of a cylindrical acrylic column with an inner diameter of 5 cm and a height of 60 cm (Figure 3.3). The acrylic was 0.5 cm thick and was transparent to allow visual monitoring of the process. A jacket was used to reduce the effect of thermal changes in the environment, to keep the water feed location independent of the particle collection site at the bottom of the column, and to obtain a uniform flow profile inside the column. This jacket was also made from the same material as the column and its dimensions were 10 cm diameter and 35 cm high. The jacket surrounded the column from the middle to slightly below the bottom end, and the column and the jacket were glued together to form a single unit.

Initial columns were constructed from glass, but due to differential heating between the inner and outer cylinders, the setup broke every time except once during manufacturing; the one that survived the manufacturing stage broke after an initial set of experiments. The plates (Figure 3.4) in the column were also made of acrylic. All the plates were attached to two horizontal acrylic plates which were screwed onto two metal rods. The metal rods were attached onto the top removable disc of the column. A Key Instruments flow meter (4-600 $cm^3$/min) was used to control the flow rate of water into the column. The particles were injected into the column through clear vinyl tubing using a peristaltic pump, and a valve was positioned at the bottom of the column to collect the settled particles. The lighter/smaller particles were carried out the top of the column by the upward flowing water and the heavier particles settled down to the bottom. The top fraction from the column was collected in a 2 L Erlenmeyer flask and the bottom fraction was collected by opening the valve at the end. To study the effect of column shape, a square cross-sectional column with the same length as the cylindrical column was also studied. This column had 5.8 cm square sides and a cylindrical jacket with the same dimensions as the jacket used with the cylindrical column.

### 3.5. METHODOLOGY

Distilled water was flowed downward into the outer column, and then upward in the inner column. A concentrated slurry of glass particles (glass spheres, 6-30 microns

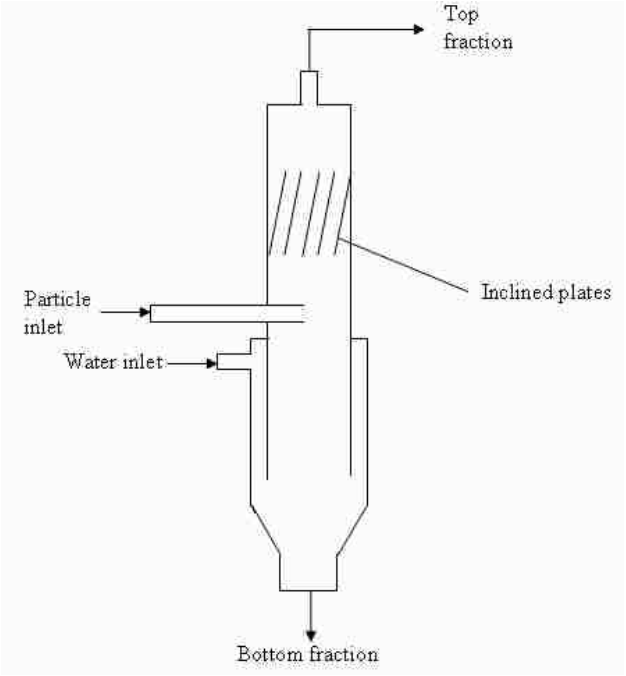


Figure 3.3 Inclined Reflux Plates in Fluidized Bed

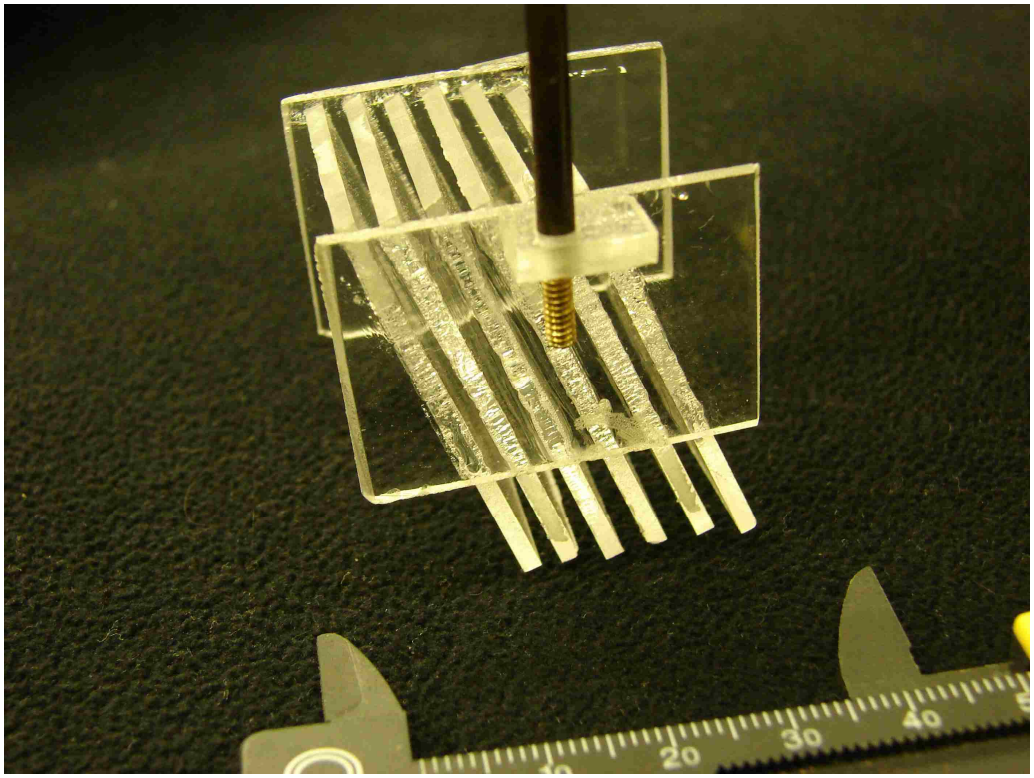


Figure 3.4 Plates

Mo-Sci. Corp., Rolla, MO) was injected into the center of the inner column through a steel inlet port. The water flow rate was adjusted just above the settling velocity of the target particles so that those larger than the desirable size ($>d_p$) settled to the bottom of the column and were collected as the bottom fraction, and particles less than or equal to the desirable particle size ($\leq d_p$) were collected as the top fraction. The valve at the bottom of the column allowed for the controlled removal of the larger fraction and prevented the flow of water out the bottom of the column during operation. The particles in the top fraction were concentrated by allowing them to settle and then siphoning out most of the superficial water. The particles from bottom fraction were collected by opening the bottom valve. The samples from the top and bottom fractions were then analyzed for particle size distribution.

## 3.6. PARTICLE SIZE DISTRIBUTION MEASUREMENTS

**3.6.1. Horiba Capa 700 Particle Size Distribution Analyzer.** Initially, a Horiba Capa 700 particle size distribution analyzer was used to analyze the particle size distributions of the top and bottom fractions from the column. The method of analysis for the Horiba Capa 700 is light penetration, which can work in two modes: gravity settling and ultra-centrifugal settling. The instrument can measure the size distribution of particles from 0.01 to 300 μm quickly and with a high degree of precision. It has six different settlement modes, ranging from settlement by ultra-centrifuge at 10,000 RPM (roughly 9,000 G) to natural settlement (settling under the influence of gravity). The Horiba gave only a volume-based distribution and eventually had maintenance problems that prevented further use, so it was necessary to search for another particle size distribution analyzer.

**3.6.2. Laser Diffraction.** In laser diffraction, a sample of particles passes though a broad beam of laser light, and the incident light is scattered onto a Fourier lens, which focuses the light onto a detector array. An inversion algorithm is then used to obtain the particle size distribution from the gathered diffracted light data. Two particle size analyzers that worked on laser diffraction principle were used: 1) Beckman Coulter LS Particle Size Analyzer, located at Mo-Sci Corp with capability of measuring particle sizes ranging from 0.04 μm to 2000 μm. Both wet and dry samples can be analyzed for

particle size. 2) Microtrac S3500, which has the capability to analyze a range of particle sizes from 0.024 µm to 2800 µm and can also analyze non-spherical particles. The laser light for the analysis is provided by three fixed solid-state lasers that have computer-controlled single lens alignment[27].

The operating procedure for the Microtrac S3500 was less tedious and simpler than the Horiba CAPA 700. A sample delivery control unit was piped to a distilled water source, which was the inlet for distilled water to the system. The Microtrac automatically ultrasonicated the samples, diluted them if necessary, and analyzed them for size.

# 4. MODELING USING CFD

## 4.1. INTRODUCTION TO CFD

Computational fluid dynamics (CFD) is the method of using computational or mathematical techniques to study the flow of a fluid. Fluid flow profiles of simple flow systems as well as complicated systems involving chemical reactions, mechanical movement, or heat or mass transfer can be predicted quantitatively with ease by using CFD. In it, the system can be virtually built and then the real-life conditions may be applied to study it.

In this work, CFD was used as a preliminary method to analyze the flow patterns for different flow rates. The velocity profile of the flow through the column was investigated to estimate what was expected when the actual experiments were carried out. The CFD software chosen was COMSOL 3.1 (formerly known as FEMLAB).

## 4.2. COMSOL 3.1.

The procedures to build model geometries in COMSOL are simple and both 2-D and 3-D geometries can be created. Different variables and equations can be defined and used within a model. The material library can be customized, equations on multiple geometries can be linked, the model mesh can be fine-tuned, and the problem can be solved and the solution post processed. COMSOL solved a fluid problem by solving the Navier-Stokes equation.

**4.2.1. 2-D Modeling of Upward Flow Through a Tube.** A simple 2-D model of upward flow of water through a tube of the same dimensions as the experimental system was used to roughly study the expected flow profiles in the column. The input flow rate corresponded to the settling velocity of a 10 μm particle and the boundary conditions were set to match the experimental conditions. The velocity profile obtained is shown in Figure 4.1. It can be seen that the maximum velocity occurs at the center and diminishes towards the walls (parabolic velocity profile) at the walls, as expected.

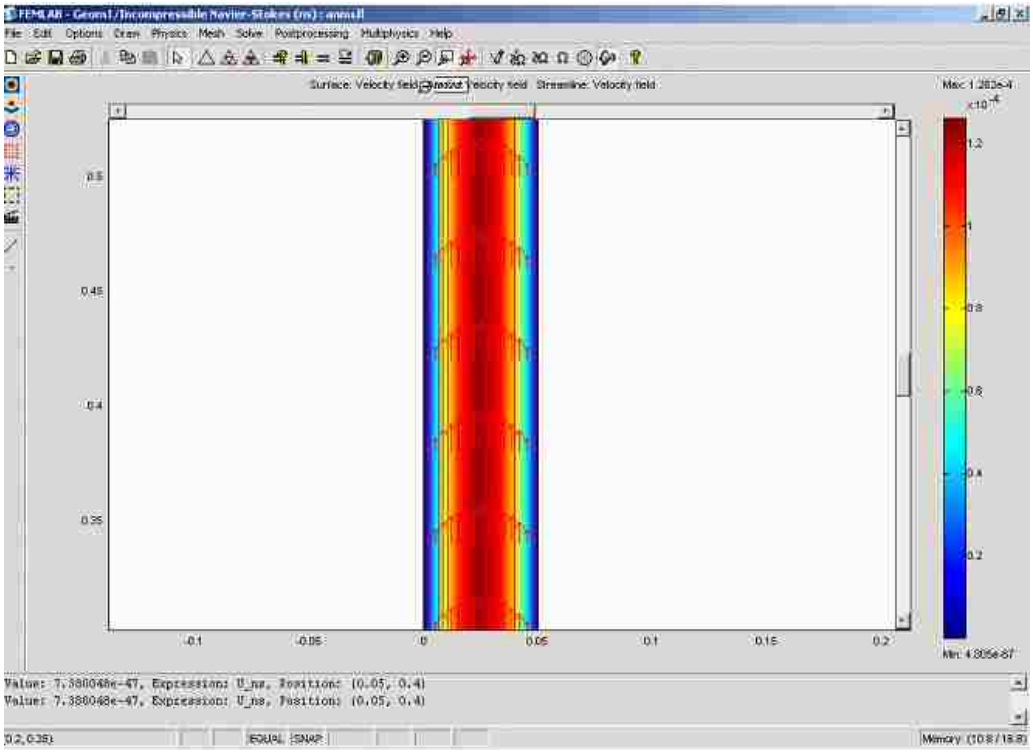

Figure 4.1 Velocity Profile for Fluid Flow at the Settling Velocity of a 10 µm Particle

Flow rates corresponding to settling velocities of other particles sizes were also modeled. However, since the smaller particles were targeted and the velocity profile for the smallest particle size was more relevant, only the profile of the 10 µm particle system is given here.

**4.2.2 2-D Modeling Upward Flow of Water Through Tube with Constricted Exit and Particle Injection Port**. After the velocity profile for the upward flow of water was obtained, the constriction at the top of the column and the particle injection port were added to the model (Figure 4.2) to understand their effect on the velocity profile.

The velocity profile was obtained by applying the boundary conditions and specifying the domain and sub-domains. Figure 4.3 shows the velocity profile for flow with velocity as that of the settling velocity of 10 µm particle with constricted exit and particle injection port .The solution obtained (Figure 4.3a) gave a general flow profile in the column and upon further magnification (Figure 4.3b) the velocity profile near the constricted exit was seen.

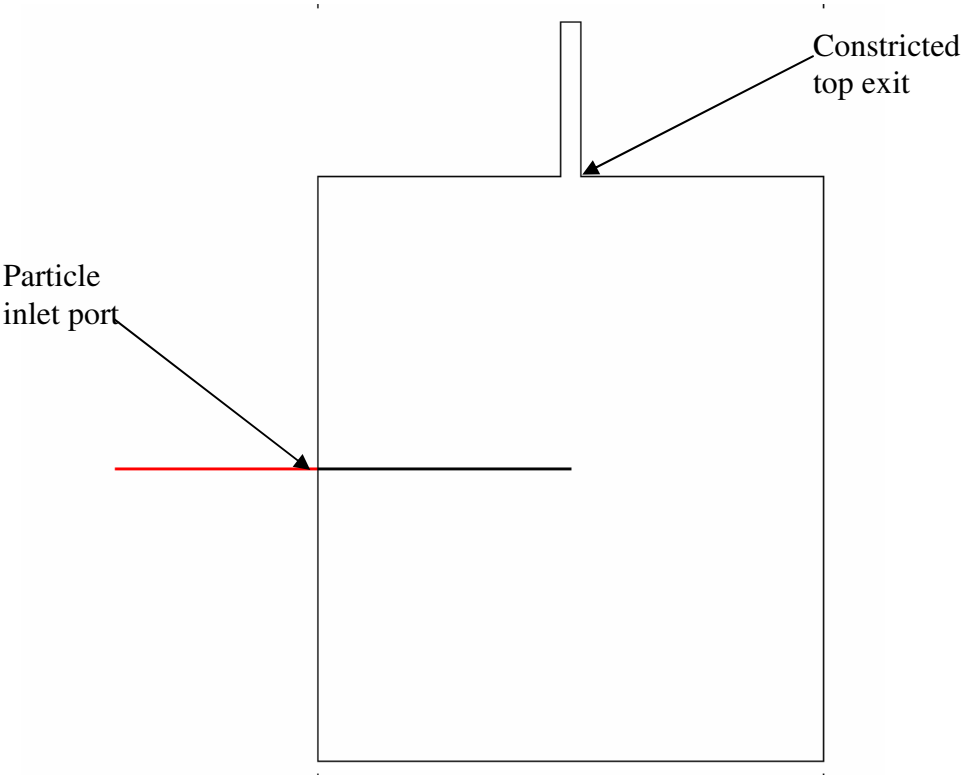


Figure 4.2 COMSOL Geometry before Solving

The flow through the particle inlet did not seem to have any effect at all on the velocity profile inside the column (Figure 4.4). The constriction at the top exit had a velocity almost a magnitude greater than the velocity in the pipe, which was expected.

**4.2.3. 3-D Modeling of the Experimental Setup (Circular Cross-Section).** Creating a 3-D geometry was more complicated than creating a geometry in two dimensions (Figure 4.5). In addition, after the geometry was created in 3-D (Figure 4.5a), it was not easy to solve the model in COMSOL as the computer ran out of memory during processing. To overcome this challenge, the geometry was sliced at the line of symmetry and one half was solved. This reduced the load on the software by half and the CFD model yielded a solution showing the velocity profile in 3-D (Figure 4.5b). The solution obtained showed that the particle injection port did not have any effect on the flow pattern, which is consistent with the result obtained from the 2-D model.

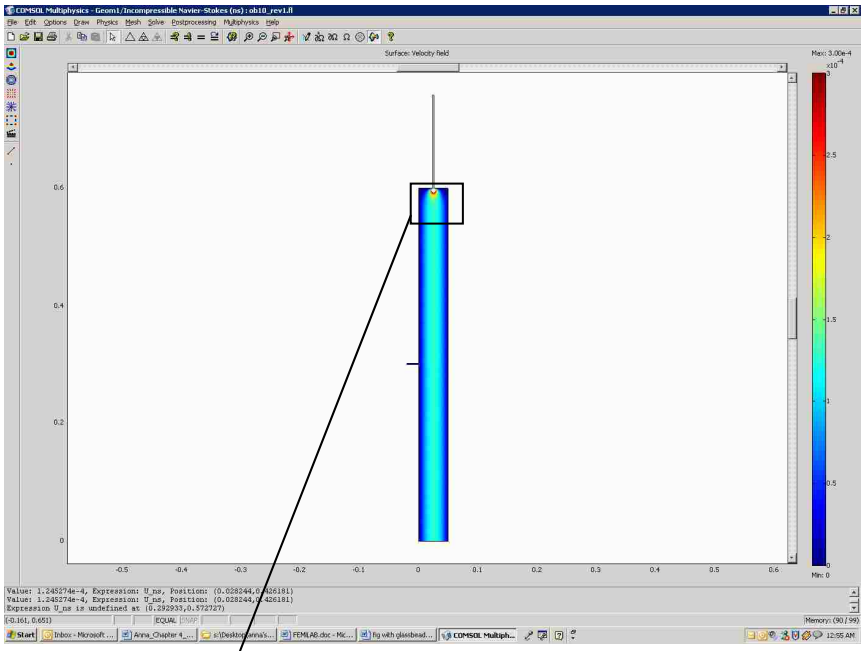

a) Solution

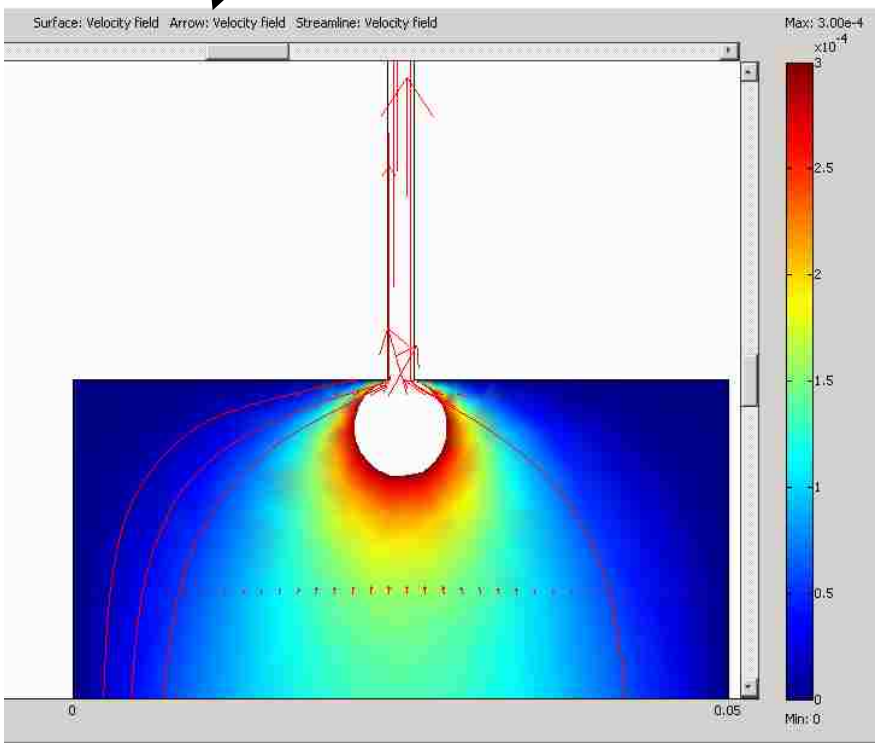


b) Magnified View near the Exit

Figure 4.3 Velocity Profile for Flow with Velocity as that of the Settling Velocity of 10µm Particle with Constricted Exit and Particle Injection Port

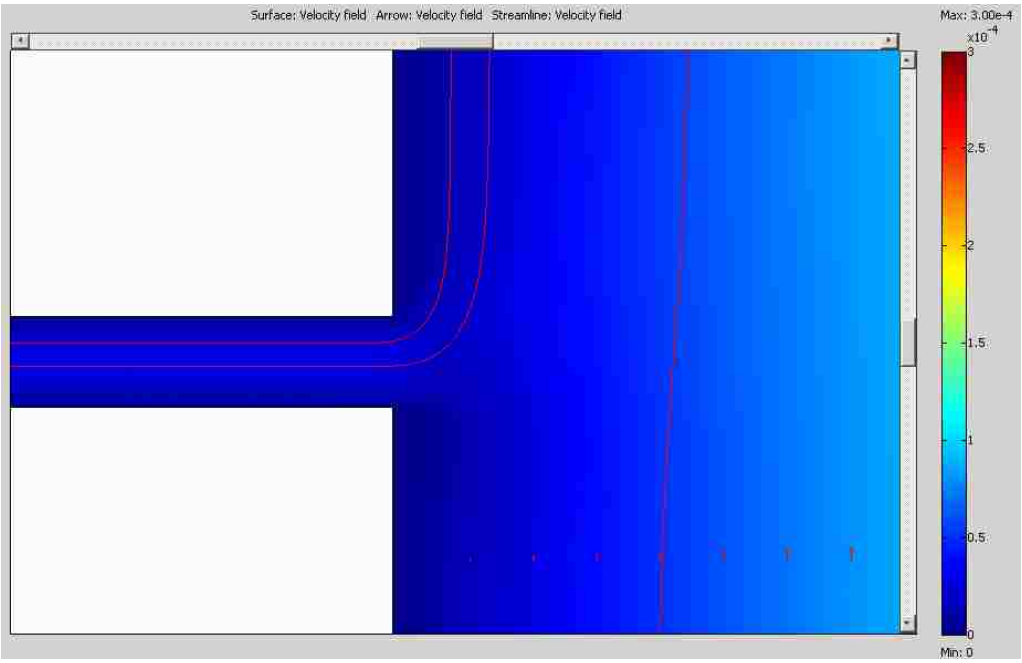


Figure 4.4 Velocity Profile for Flow at Particle Injection Port (Magnified View)

On analysis of the CFD solution, it is clear that the maximum velocity was seen at the water inlet in the jacket and as the water traveled downward, the velocity decreased until a uniform velocity was reached. It is seen from Figure 4.6 that the particle inlet port did not have any effect on the flow profile inside the column. The analysis also verified that a uniform flow entered the inner column and appeared to be uniform throughout the width of the column, rather than having a parabolic velocity profile like the solution from the 2-D model. However, this is an artifact of the wide scaling of velocities, and the parabolic velocity profile is more visible in the arrow plot shown in Figure 4.6b. The solution seen in Figure 4.6b also illustrates that the fluid in jacket was not stagnant and that it circulates around the jacket as expected.

**4.2.4. 3-D Modeling of the Experimental Setup (Square Cross-Section).** To study the effect of column shape on classification efficiency, an experimental setup with a square cross-section was studied. The solution obtained showed that the column cross-section does have some effect on the flow pattern. The geometry for the column with a square cross-section was created in the same way as that for the column with circular cross-section. Figure 4.7 shows the velocity the #-D

geometry and the velocity profile in a column with square cross-section. Figure 4.7a shows the geometry of the column with square cross-section and Figure 4.7b shows the velocity profile after the CFD model was solved. The flow profile at the water inlet is slightly different from that in the cylindrical column and this difference can be attributed to the square column having edges and corners unlike the symmetric cylindrical column. The other differences in flow profile are not as evident because the scale is too wide.

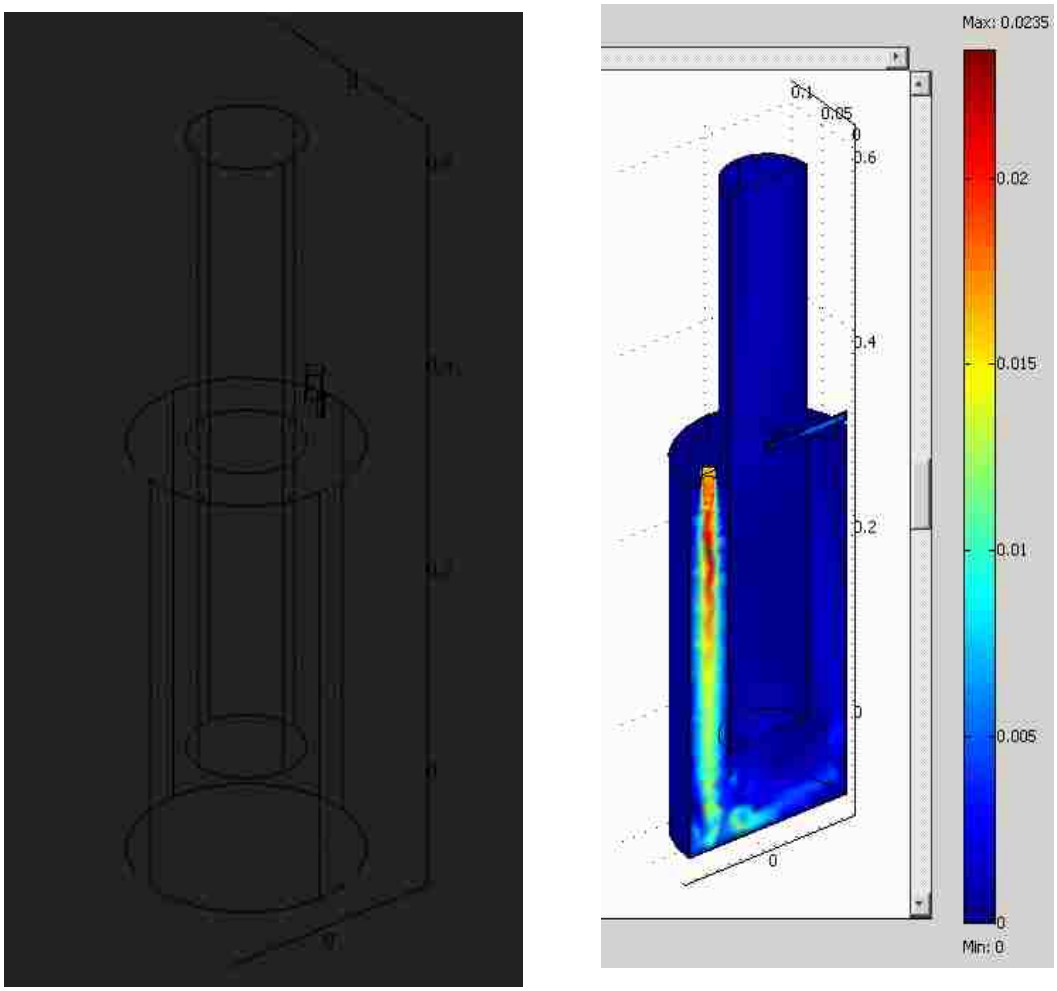


a) 3-D Geometry b) Velocity Profile

Figure 4.5 3-D Geometry and Velocity Profile (Circular)

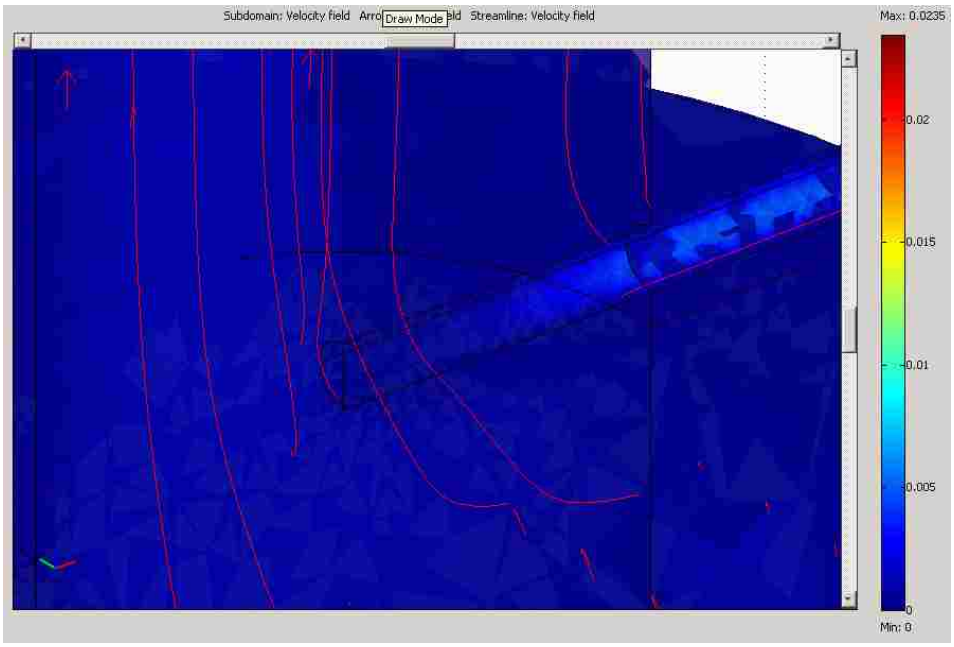


a) Flow near the Particle Injection Port

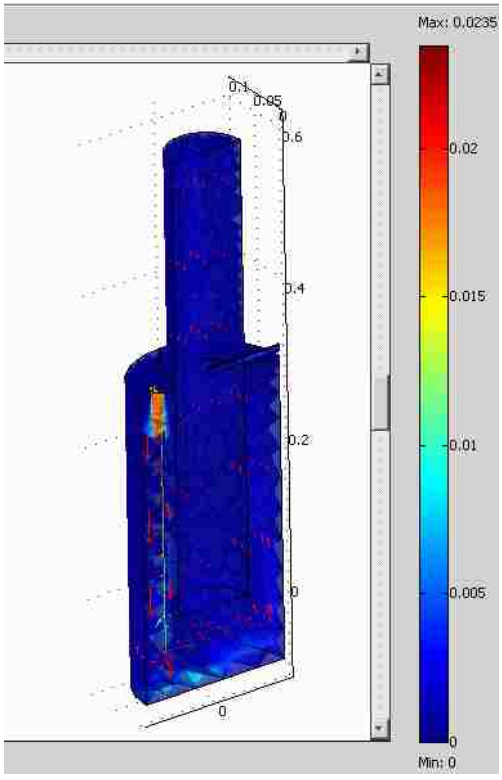


b) Arrow Plot Showing Parabolic Flow Profile

Figure 4.6 Magnified View of Flow near Particle Injection Port and an Arrow Plot

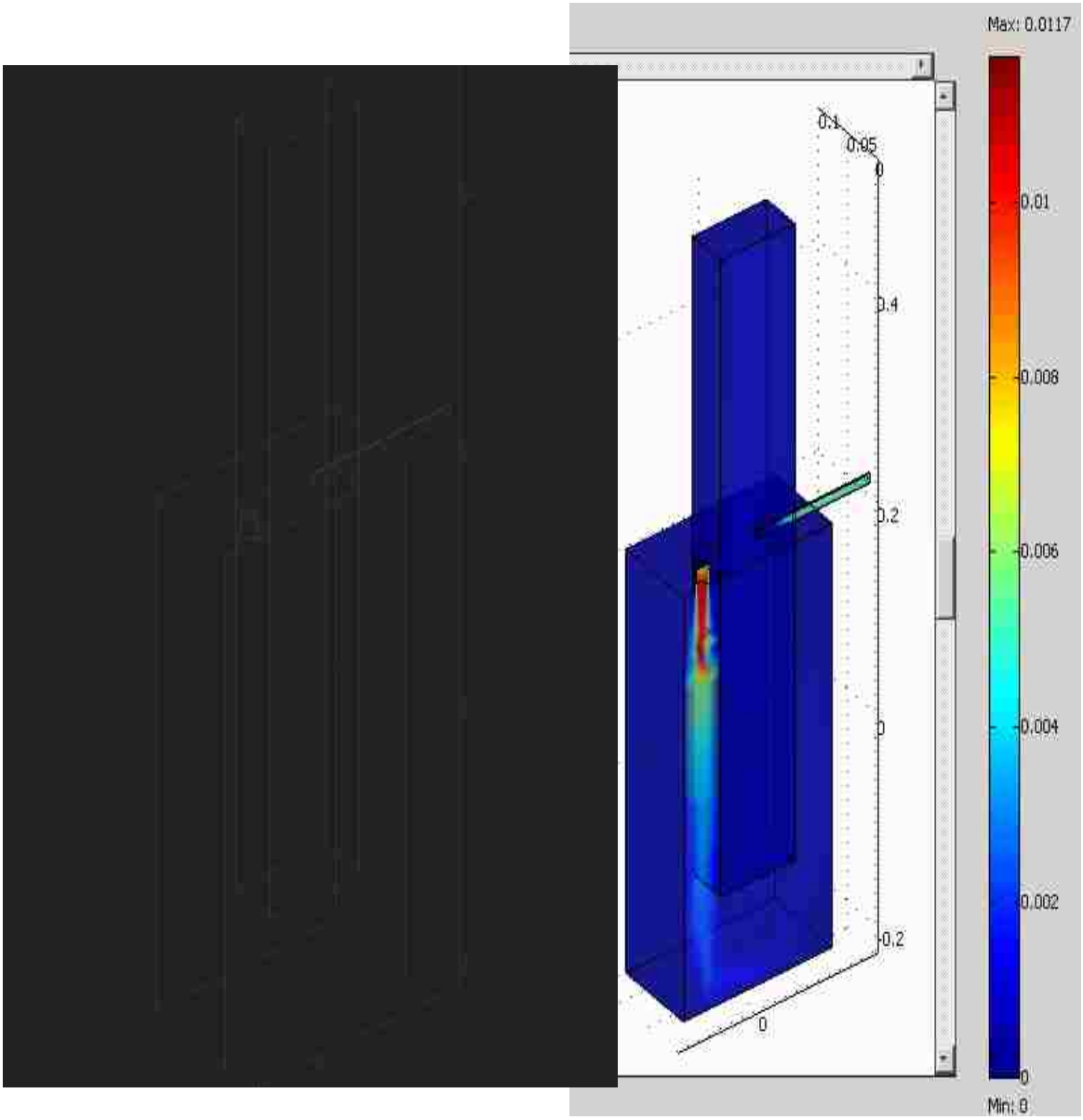


a) 3-D Geometry

b) Velocity Profile

Figure 4.7 3-D Geometry and Velocity Profile (Square)

It was clear from the solution obtained that the maximum velocity occurred at the water inlet in the jacket. As the water traveled downward, the velocity decreased until a uniform velocity was reached, which is similar to the solution obtained from the cylindrical column. Due to effect of the corners and edges, the flow looked different near the particle injection port (Figure 4.8), although the port did not seem to have any effect

on the flow profile. On plotting an arrow plot as in Figure 4.8b, the parabolic velocity profile can be seen.

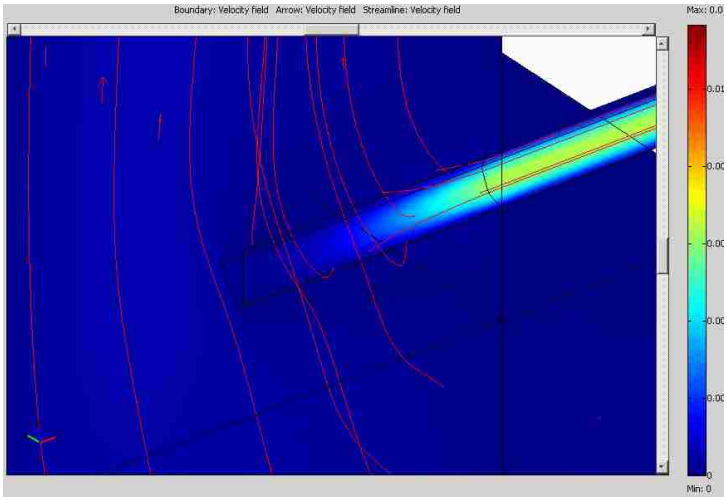


a) Flow Near the Particle Injection Port

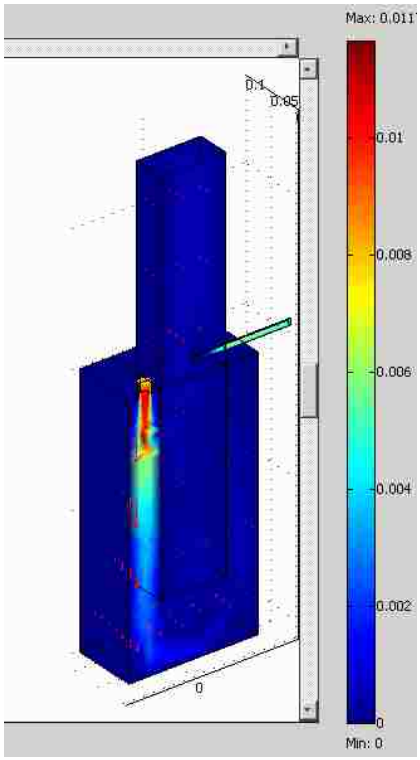


b) Arrow Plot Showing Parabolic Flow Profile

Figure 4.8 Magnified View of Flow near Particle Injection Port and an Arrow Plot

# 5. RESULTS AND DISCUSSION

## 5.1. INITIAL EXPERIMENT

Initial settling experiments were carried out using blue cobalt glass spheres to study whether size classification could be achieved by the classification technique that was proposed. A separation into distinct top and bottom fractions was noted, so it was concluded that particle classification was possible and for further experiments the colorless glass spheres were used. Next, a water flow rate of 35 $cm^3$/min was set (the flow rate required for the settling of a 10 µm particle in water). The fraction of particles less than 10 µm in the feed was very small, so the volume of overflow was insufficient to measure a particle size distribution. As a result, the flow rate of water was increased to 50 $cm^3$/min, which corresponded to a cut size of ~24 µm. Samples from the top and bottom fractions were sent to Mo-Sci for analysis.

The particle size distribution curves showed three peaks for the top fraction, one peak for the bottom fraction, and two peaks for the pure feed (Figure 5.1), and although a separation was noticed, it was not significant. Particles sizes larger than those in the feed were found in the top fraction because of agglomeration, so a surfactant (Tween 80) was used to prevent this in all future experiments. The top fraction was examined under a microscope and some angular pieces were found along with the glass beads (Figures 5.2a and 5.2b). This may have been the reason for the multiple peaks in the particle size distribution. The bottom fraction and the feed were then tested for angular pieces. No angular pieces were found in the bottom fraction but they were present in the feed. Upon investigation on the angular pieces, it was found that these angular pieces were frits, whose origin lies in the precursor used for production of glass beads at Mo-Sci. Glass beads were manufactured at Mo-Sci by melting broken glass (the precursor was procured from various industries), and those pieces that were not completely melted remained in the feed as frits. To remedy this, a new feed with the same particle size range (3-60 µm) free from frit was used for all further experiments.

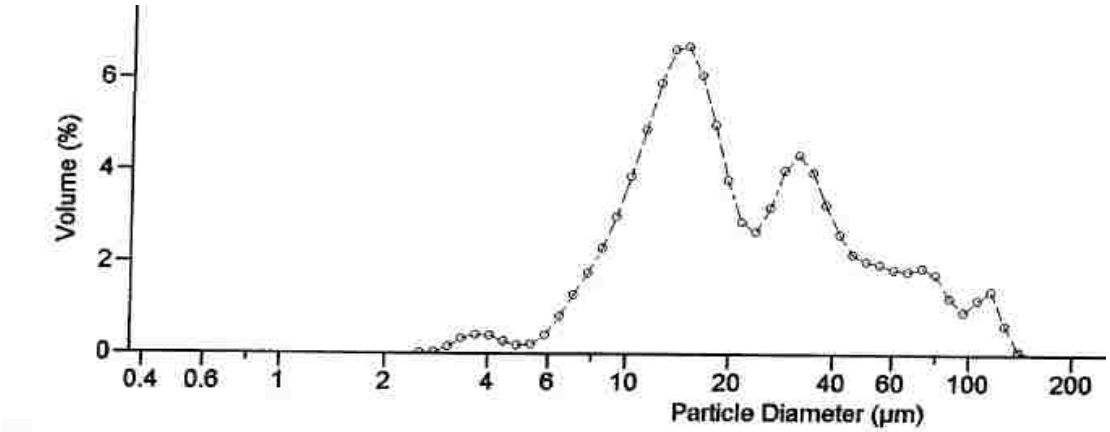


a) Top Fraction

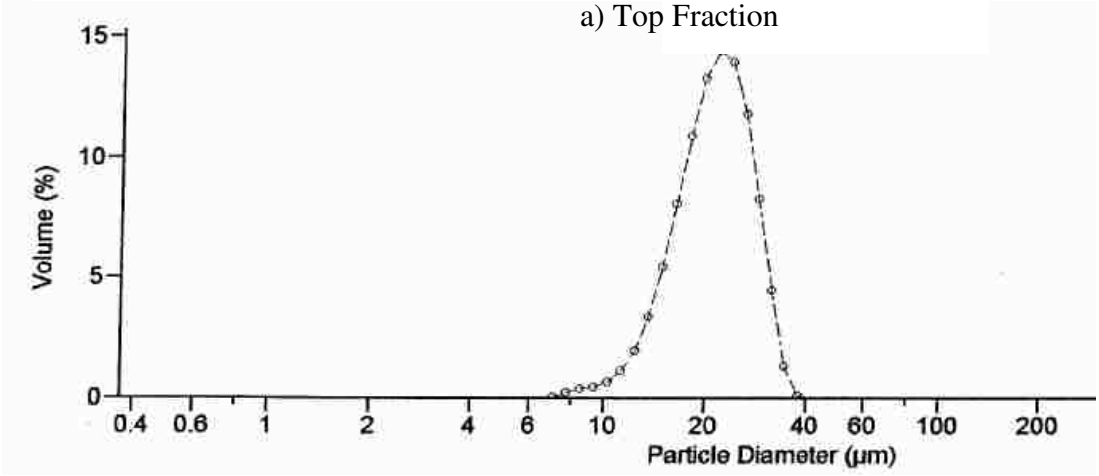


b) Bottom Fraction

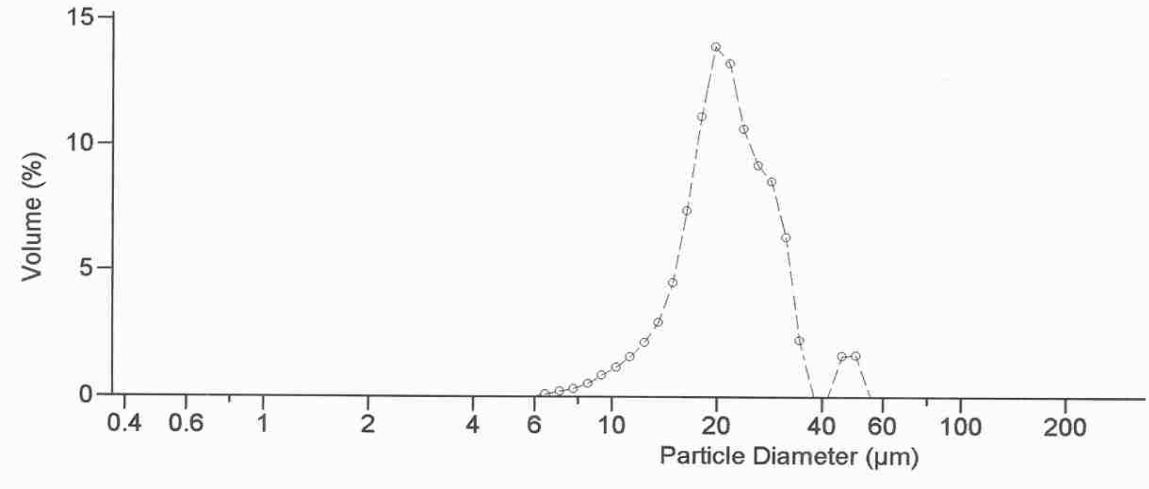


c) Feed

Figure 5.1 Particle Size Distributions

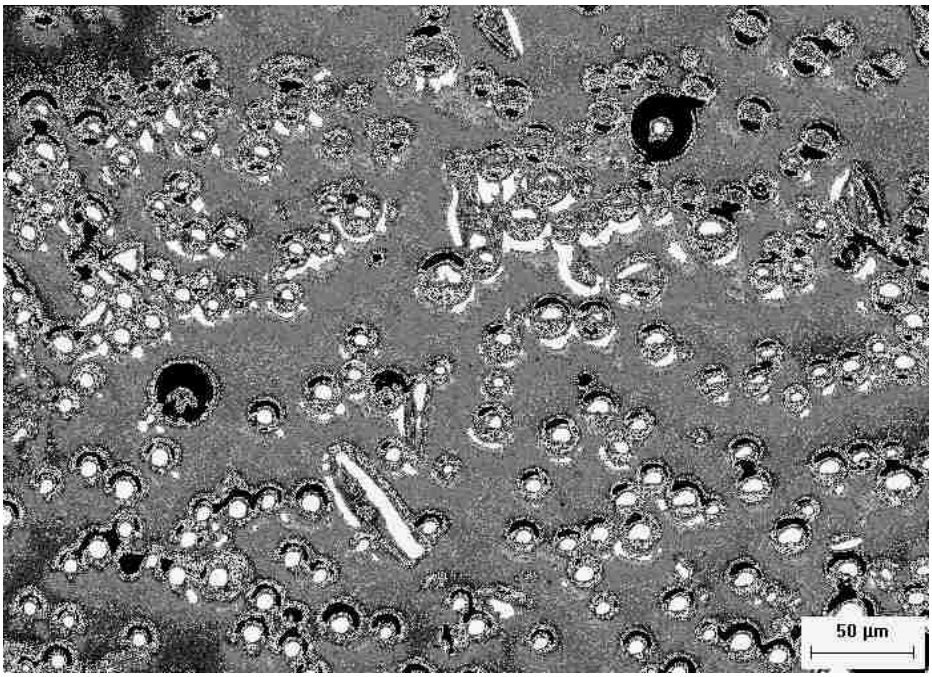


a) Top Fraction

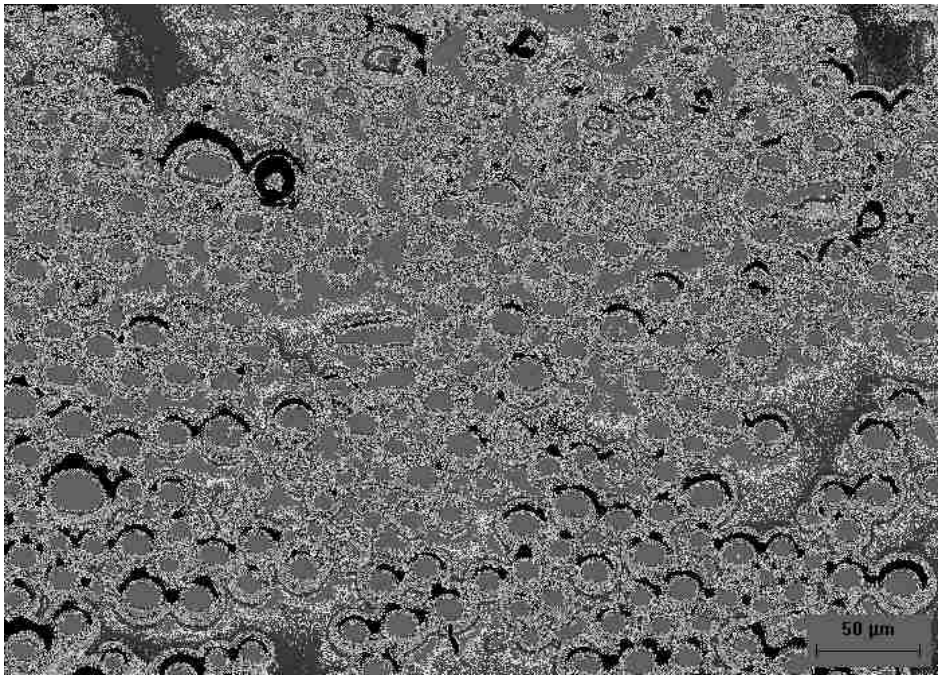


b) Bottom Fraction

Figure 5.2 Top Fraction and Bottom Fraction

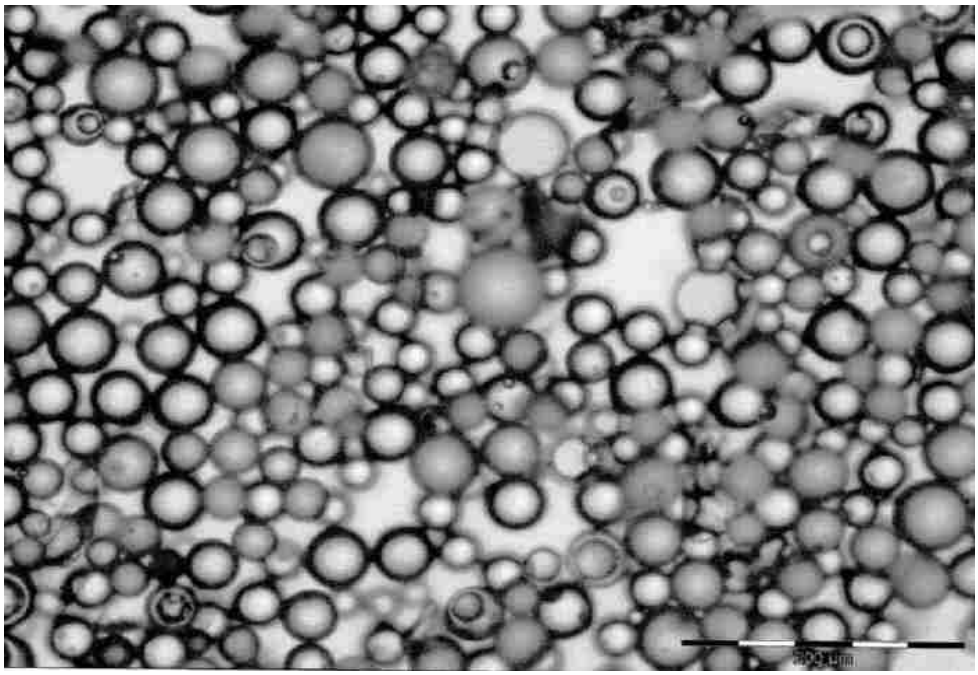

a) Feed without Frit (New feed)

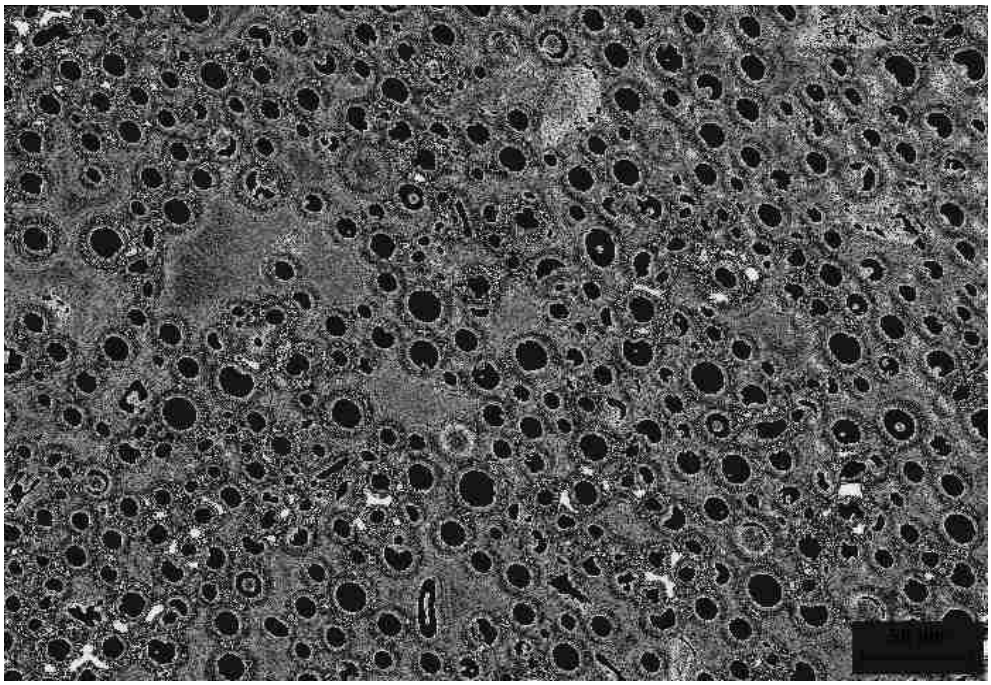

b) Feed with Frit (Old feed)

Figure 5.3 Feed With and Without Frit

## 5.2. EFFECT OF WATER FLOW RATE

The effect of water flow rate on separation was studied in the cylindrical column by varying the flow rate of water from 50 CCM to 200 CCM. Figures 5.4a and 5.4b represent the data obtained. The term "initial" in Figure 5.4a refers to the mean diameter of the feed and the bars represent the standard deviation (experimental error) from the mean of the five experiments carried out at each point. Figure 5.4b shows the effect of the water flow rate on separation. This separation is the difference between the mean diameters of the bottom fraction/underflow (Bottoms) and the top fraction/overflow (Tops). It is seen that as the flow rate of water is increased from 50 CCM to 200 CCM, the separation efficiency decreases to the point of almost no separation at all, which was expected. As the flow rate of water is increased the cut off diameter of the particles increases.

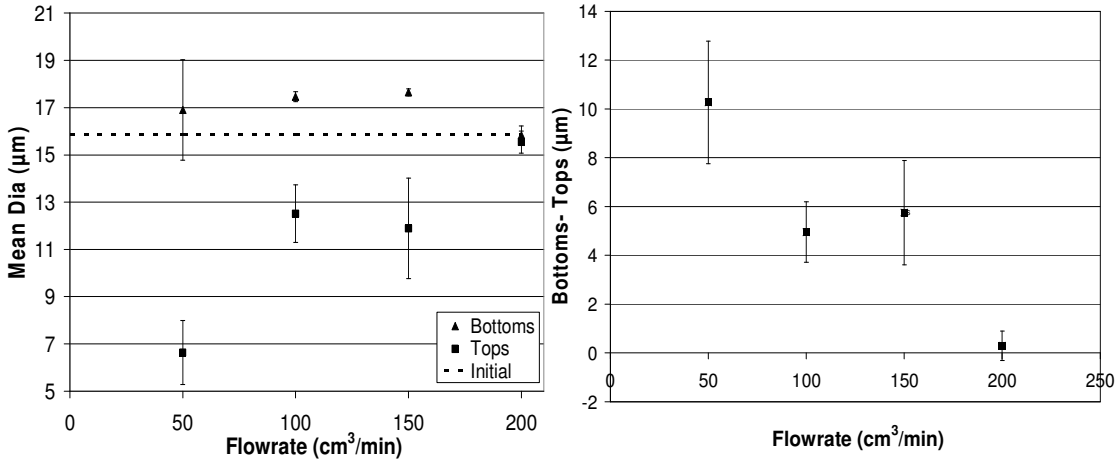


a) Mean Diameter

b) Separation

Figure 5.4 Effect of Water Flowrate

## 5.3. EFFECT OF PARTICLE FEED RATE

The effect of particle feed rate was studied by varying the inlet particle mass flow rate from 0.78 g/min to 16 g/min (Figures 5.5a and 5.5b). The peristaltic pump used to

feed the particles could feed particles at a maximum rate of 16 g/min. The effect of particle feed rate on separation was negligible because the concentration of particles in the column was very dilute across the entire range of particle feed rates. The porosity or voidage of the entire column was 99.45% when 16 g of particles were present in the column.

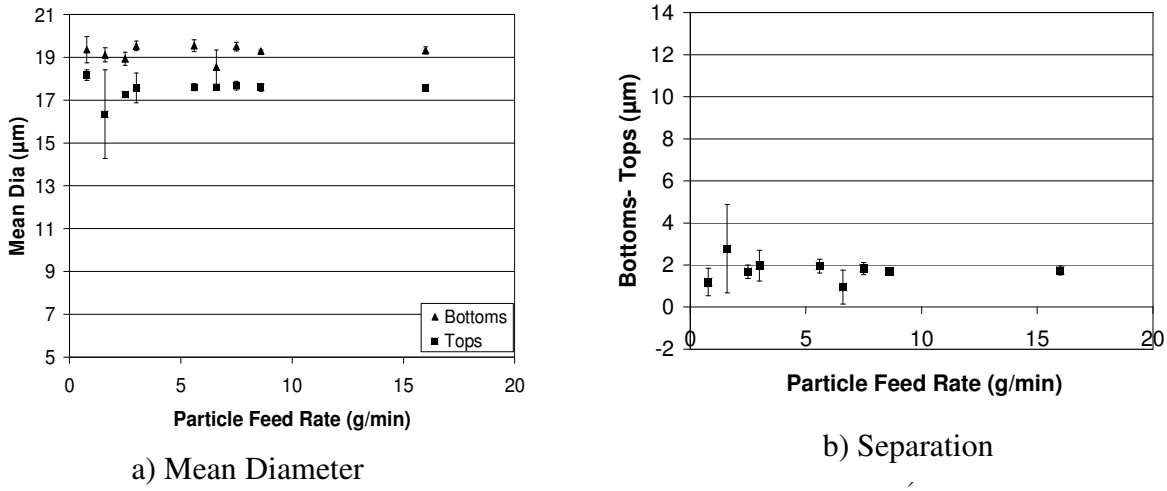


a) Mean Diameter

b) Separation

Figure 5.5 Effect of Particle Feed Rate

## 5.4. EFFECT OF NUMBER OF PLATES

The effect of the number of plates was studied by keeping the plate angle and length constant at 60 degrees from the horizontal and 1.625 inches, respectively. The spacing between the plates decreased as the number of plates was increased. Experiments with 2, 4, and 6 plates were performed, and Figure 5.6 shows that the number of plates did not have much of an effect on separation. This may be due to the limited range of plate numbers considered (0-6 plates).

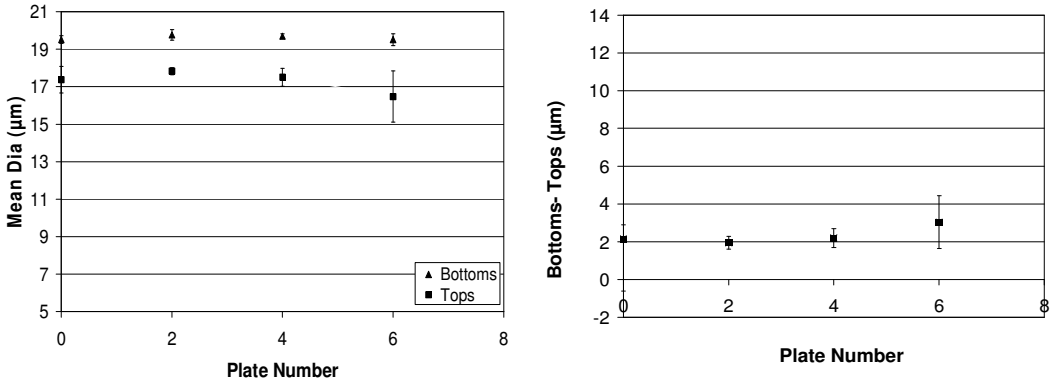


a) Mean Diameter

b) Separation

Figure 5.6 Effect of Number of Plates

## 5.5. EFFECT OF PLATE ANGLE

The effect of plate angle on separation was studied by using two plates with a constant length of 1.625 inches. The angles studied were 45, 60, and 75 degrees from the horizontal and the data are presented in Figure 5.7. It can be concluded that the angle of plates did not have a significant effect on the separation over the range of angles considered here.

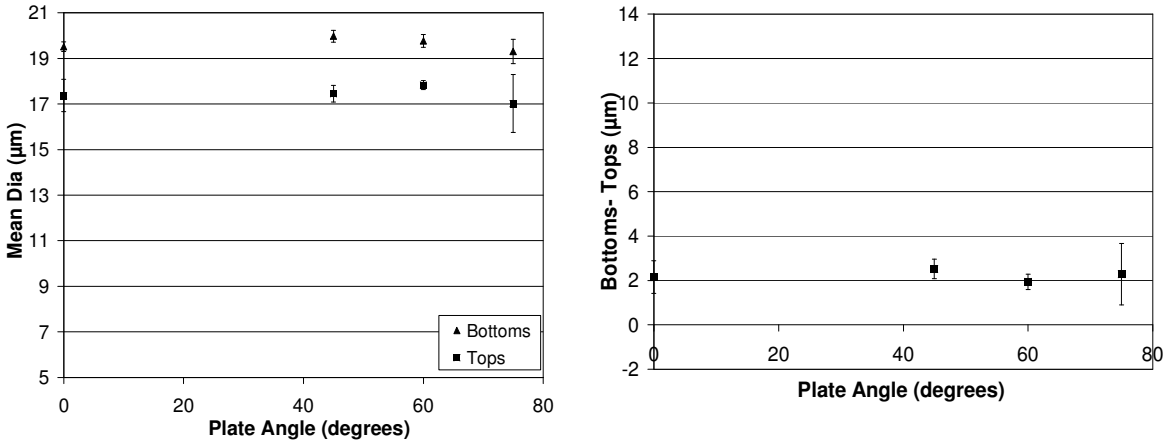


a) Mean Diameter

b) Separation

Figure 5.7 Effect of Plate Angle

## 5.6. EFFECT OF PLATE LENGTH

The effect of plate length on separation was studied by using 8 plates at a constant angle of 87 degrees from the horizontal. Figure 5.8 shows the effect of plate length on separation. The lengths of plates used were 2, 3, and 4 inches. From Figure 5.8 it can be

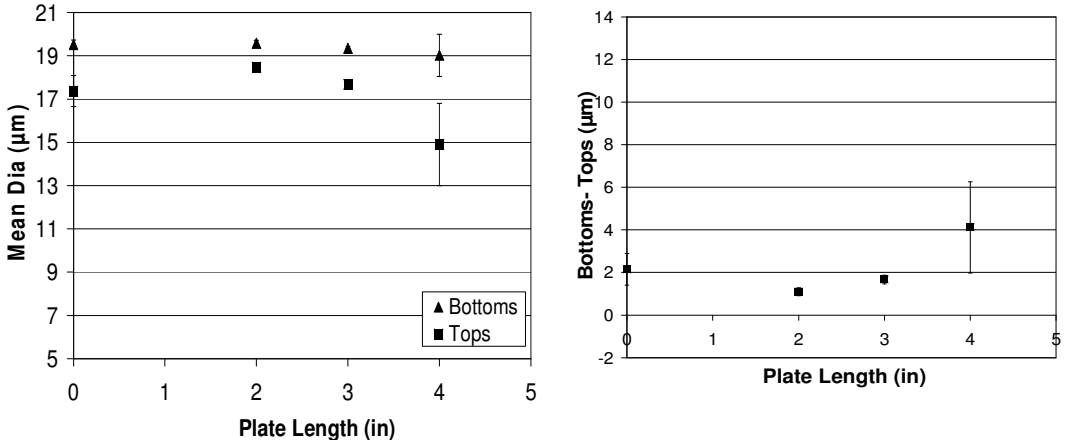


a) Mean Diameter b) Separation

Figure 5.8 Effect of Plate Length

concluded that as the length increases there was a slight increase in separation. It is seen from Figure 5.8a that there is a maximum at the two plate condition and a minimum in Figure 5.8b at the same point. This trend may be attributed to the fact that at a plate length of 2 inches, the plates may hinder the flow without any increase in sedimentation area. By increasing the plate length, the effective sedimentation area available for the particles to settle is increased, which leads to an improvement in separation.

## 5.7. EFFECT OF COLUMN SHAPE

The effect of column shape on separation was studied by comparing results from a rectangular column (square cross-section) and circular column (circular cross-section). The columns were used with and without plates at different angles, and Figure 5.9 shows

no evident effect of column shape on separation. From the figure, there is no noticeable separation for systems containing no plates and with plates at 60 degrees and 75 degrees; however, at a plate angle of 45 degrees, the circular column yielded better separation than the rectangular column. This worsened separation in a square column at 45 degrees may be due to the effect of the corners on the flow profile, which is absent in the cylindrical column and probably is negated at larger angles. This angle exactly bisects the cross-section of the column, but is an aspect that should be investigated in the future.

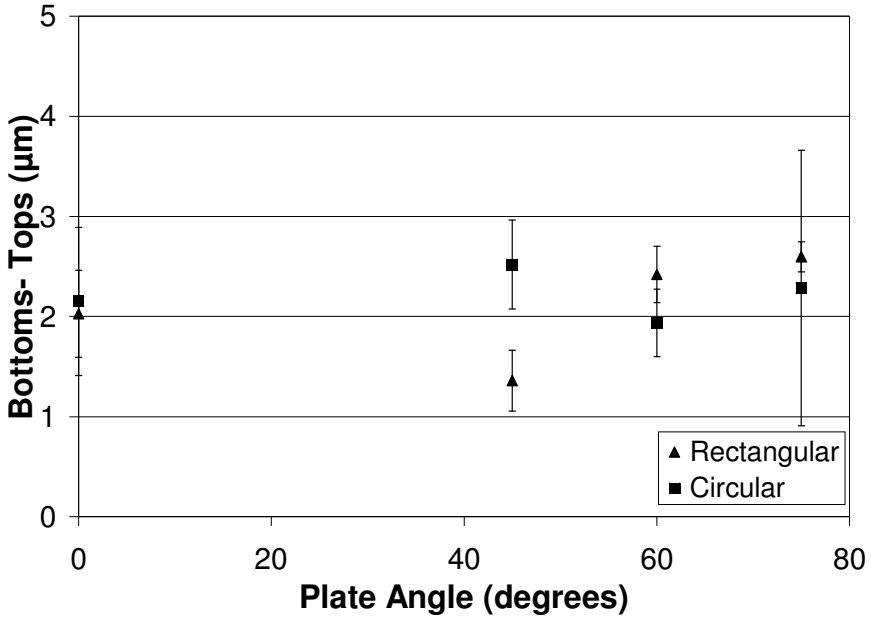


Figure 5.9 Graph Showing Separation vs. Plate Angle

## 5.8. COMPARISON OF THEORY WITH EXPERIMENTAL RESULTS

The theory developed based on multiple particle settling was found to fit the experimental system more appropriately than the one based on single particle settling. This was because of the fact that it was more than a single particle that was settling in the column, especially when it is the settling in between the plates that's being considered where the concentration of particle stay almost constant and the particles come in close

proximity to one another. The particle size distributions for the overflow and underflow obtained theoretically were compared those obtained experimentally for each analysis.

**5.8.1. Effect of Water Flowrate.** Water flowrate was found to affect separation the most. The actual cut-off diameters from experiments were compared with the theoretical cut-off diameters predicted by the Stokes equation. The results (Figure 5.10) showed that the cut-off diameter was underpredicted only by about 20% consistently. This experimental cut-off diameter was based on the assumption that both the top and bottom fractions followed a normal distribution.

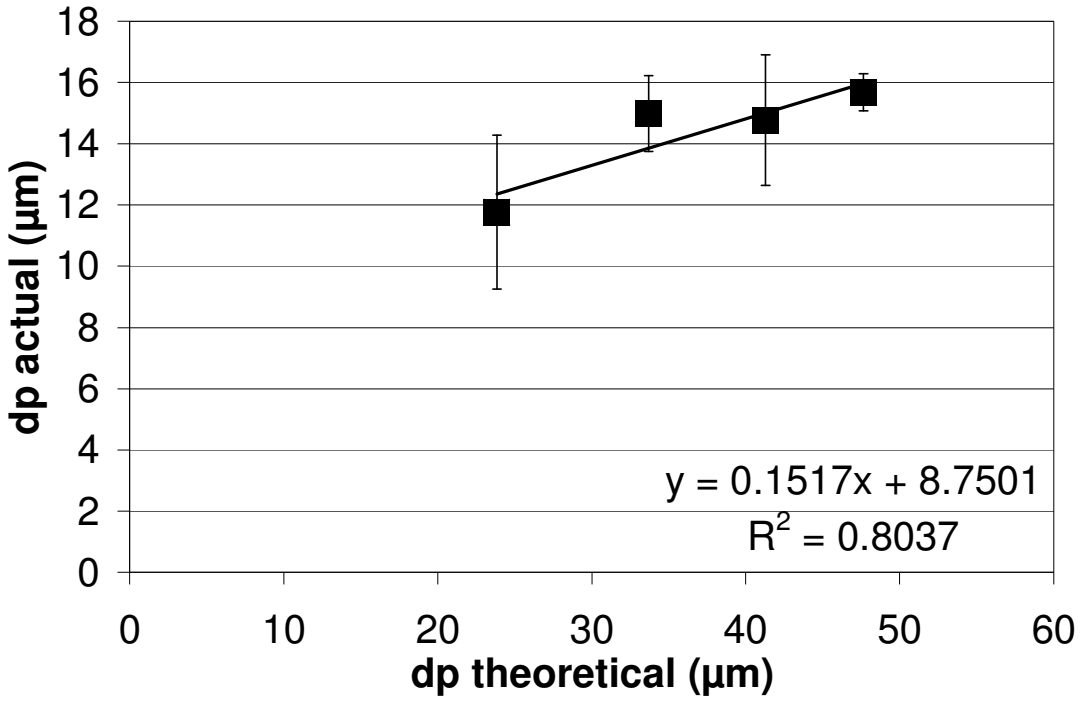


Figure 5.10 Effect of Water Flowrate on Separation

**5.8.2. Effect of Plate Length on Separation.** Figure 5.11 shows the particle size distributions of the overflow and underflow obtained experimentally and theoretically for no plates and with plates of length 2, 3, and 4 inches. From these graphs, the experimental overflow and underflow distributions are considered to be better than those predicted theoretically because the experimental distributions are narrower

than the theoretical distributions. This improvement in experimental result can be attributed to two major factors: i) for theoretical predictions, a flat velocity profile was assumed for the upward flowing fluid as opposed to an actual parabolic velocity profile between the plates, and ii) the constricted top exit was not considered while predicting the overflow and underflow theoretically. The flat profile assumed theoretically presumed that a particle in any part of the entire width of the column experienced the same upward flow velocity, while the flow profile was actually parabolic; that is, a particle near the walls experiences a lower upward flow velocity and a particle in the center of the plates experiences the maximum velocity.

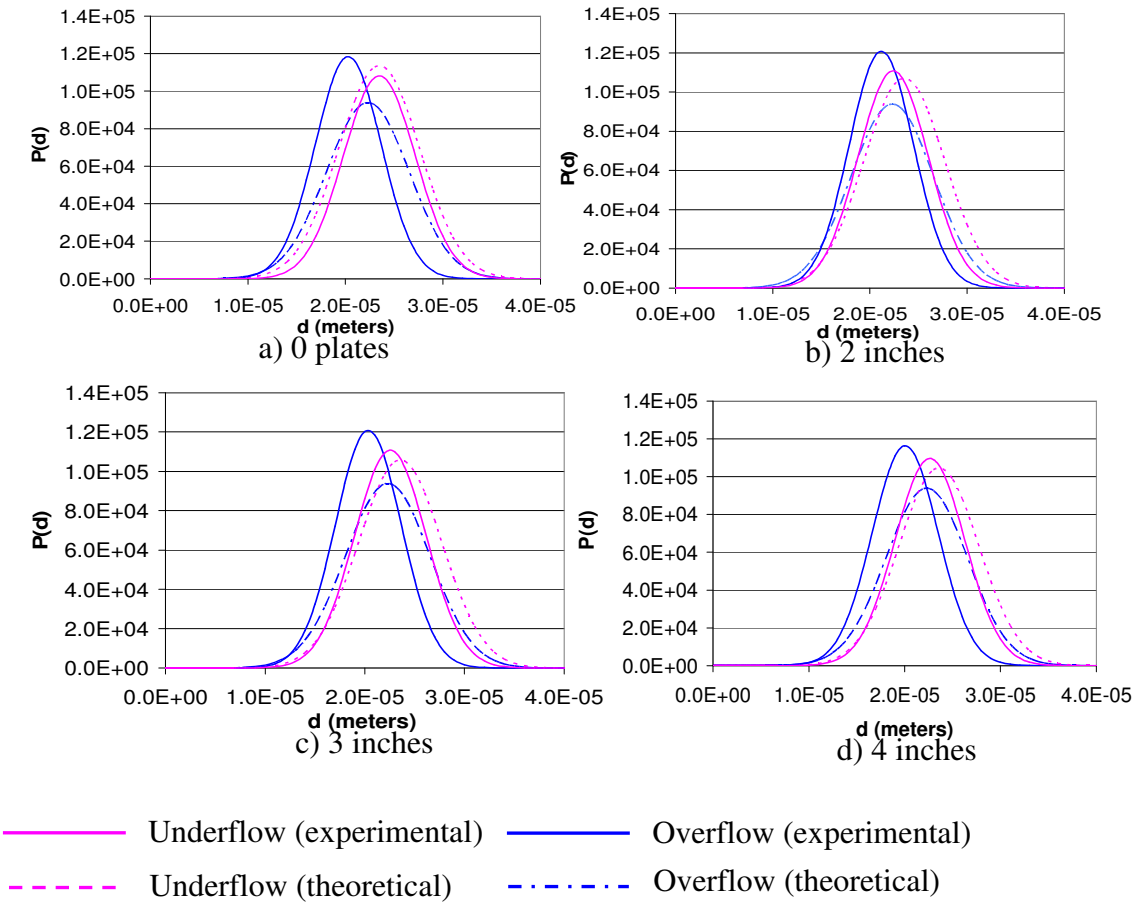


Figure 5.11 Effect of Plate Length on Separation

The constriction in the top exit resulted in a higher velocity near the top exit, which may have led to the complete removal of all the particles that reached that point. The experimental results were in good agreement with the theoretical predictions for the 2 inch plate length.

**5.8.3. Effect of Plate Number on Separation.** Figure 5.12 shows the particle size distributions of the overflow and underflow obtained experimentally and theoretically for systems with no plates and with 2, 3, and 4 plates.

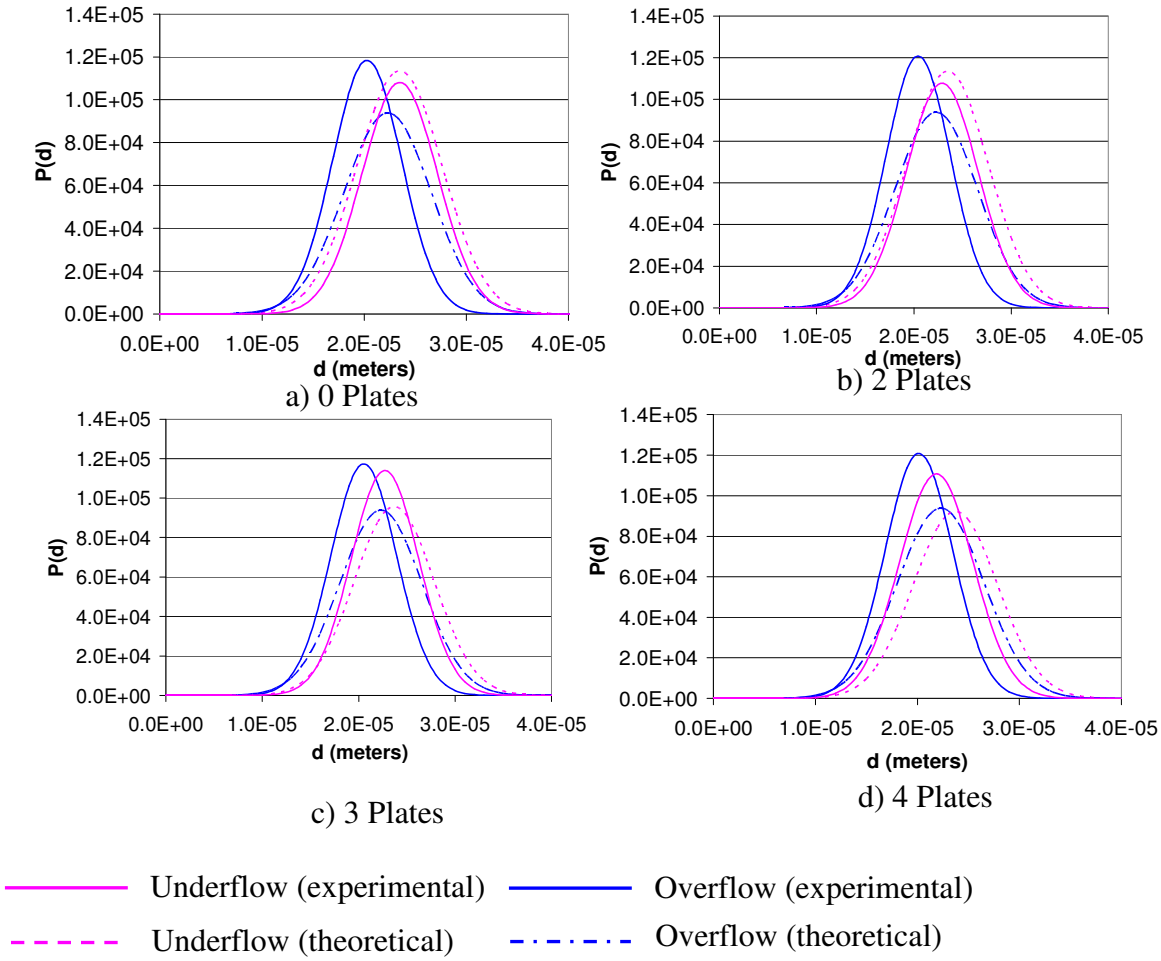


Figure 5.12 Effect of Plate Number on Separation

It is clearly seen that the experimental overflow and underflow distributions are larger in magnitude and narrower than those predicted theoretically. This improvement

in experimental result can be attributed to the same two factors discussed before. The experimental results were in good agreement with the theoretical predictions for the system containing two plates. One trend noticed here is that the theoretical predictions slightly overpredict the experimental results, as seen from the experimental and theoretical plots for the underflow in Figure 5.11b, but then underpredict for larger numbers of plates.

**5.8.4. Effect of Plate Angle on Separation.** Figure 5.13 shows the particle size distributions of the overflow and underflow obtained experimentally and theoretically with 45 degrees, 60 degrees, 75 degrees, and 90 degrees plate angles. It is clearly seen that the experimental overflow and underflow distributions are larger in magnitude and narrower than those predicted theoretically. This improvement in experimental result can again be attributed to the same two factors discussed earlier. The experimental results agreed with the theoretical predictions for the plates with a 60 degree inclination. At a 90 degree plate inclination, the theoretically predicted underflow was found to be larger in magnitude than the experimental underflow, against the trend noticed in the other graphs.

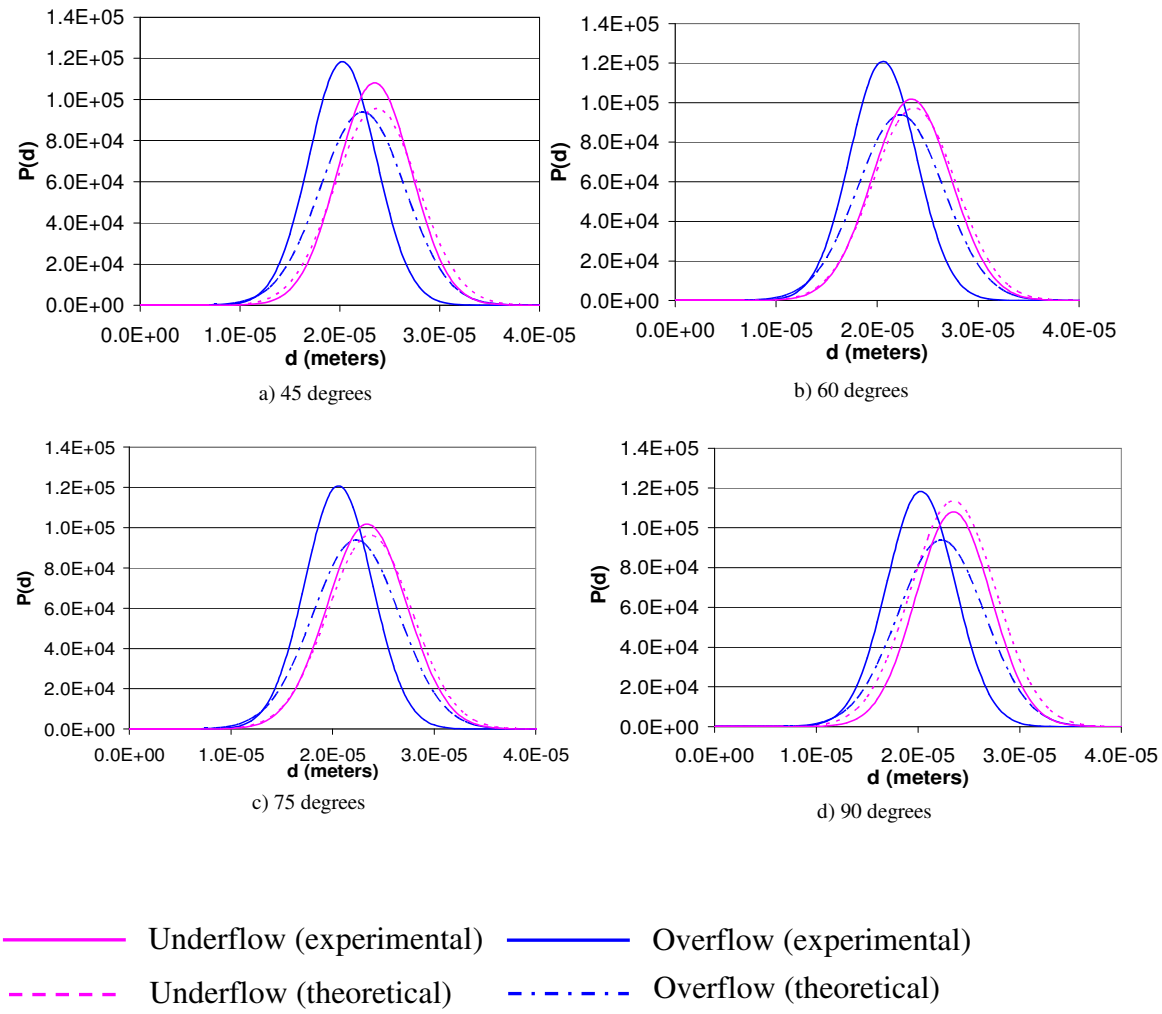


Figure 5.13 Effect of Plate Angle on Separation

# 6. CONCLUSIONS AND FUTURE WORK

The main conclusion that can be drawn from this work is that within the ranges studied the particle feed rate, plate angle, plate number, and column shape did not have a significant effect on the classification of particles. Water flow rate was found to be the most critical criterion for particle classification in this process. Particle classification based on plate length showed better efficiency for longer plates, but this must be confirmed by conducting additional experiments with a wider range of plate lengths. The circular column was found to be more efficient than the square column at a 45 degree plate inclination; under all other conditions there was no significant effect of column shape. The theory developed for the process compared well with the experimental results obtained, even though the experimental distributions were taller and narrower than theoretical predictions. The reason for this increase in effectiveness may be due to the fact that the flow profile was assumed to be flat during the development of the model instead of a parabolic flow profile as was seen in the CFD simulation. In addition, the constricted top exit of the column was not accounted for in the theoretical analysis.

One area of future work would be to use two columns in series to narrow the size distribution of the fine product. The first column removes all particles larger than the targeted particles and classification can be improved if a second column can be used to remove all particles smaller than the targeted size. In this proposed setup, the top fraction is passed to a second column which will have slightly larger dimensions than the first column (a larger dimension is necessary to control and increase the fluid flow rate), but the flow rate of water in the second column will be adjusted in such a way that all particles smaller than those with the desired particle diameter are carried out by the upward flowing water and the larger particles can be collected. A detailed sketch of the experimental set-up for future studies is given in Figure 6.1. The bottom fraction from the second column will be the desired product and the bottom fraction from the first column and the top fraction from the second column can be discarded. In addition, the effect of length of plates can be studied for larger ranges and changing the fluid properties by using other fluids with different viscosities may also be done as a continuation of this project. Larger ranges of plate numbers and plate angles must also be

investigated to conclude their effects on separation. Additional work must be also be done to verify the effect of column shape at a 45 degree inclination of plates by studying plate angles in a narrow range near 45 degrees.

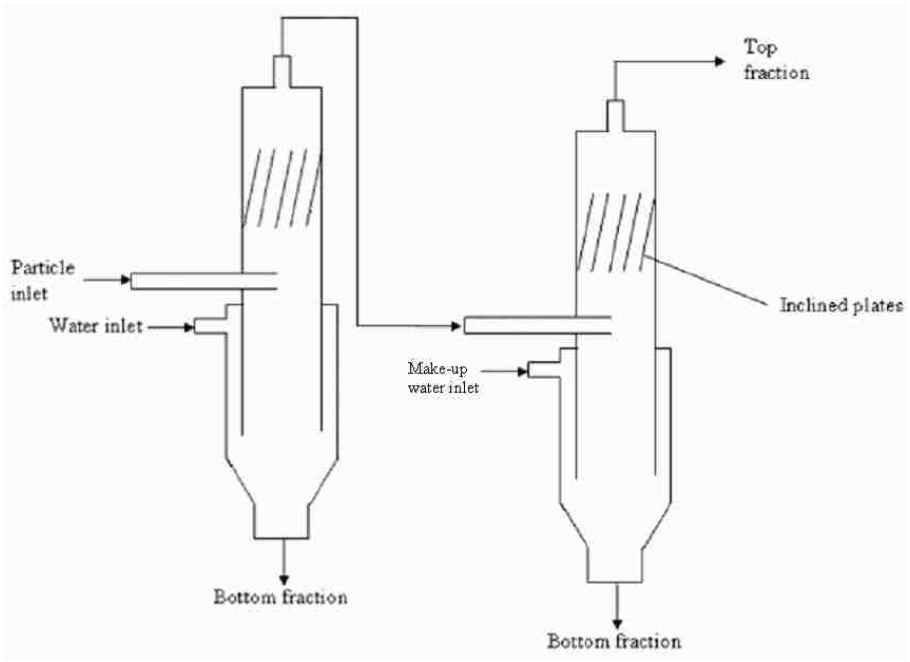


Figure 6.1 Serial Fluidized Bed Setup

## BIBLIOGRAPHY


1. Nijsen J.F.W., Van het Schip A.D., Hennink W.E., Rook D.W., Van Rijk P.P., and De Klerk J.M.H., "Advances in nuclear oncology: Microspheres for internal radionuclide therapy of liver tumours," Current Medicinal Chemistry, 9 (1), 73 - 82 (2002)

2. Armstrong D.K., Fleming G.F., Markman M., and Bailey H.H., "A phase I trial of intraperitoneal sustained-release paclitaxel microspheres (Paclimer) in recurrent ovarian cancer," A Gynecologic Oncology Group Study, 103 (2), 391 - 396 (2006)

3. Omi S., Kaneko K., Nakayama A., Akira K.K., Taguchi T., Iso M., Nagai M., and Ma G., "Application of porous microspheres prepared by SPG (Shirasu Porus Glass) emulsification as immobilizing carriers of glucoamylase (GluA)," Journal Of Applied Polymer Science, 65 (13), 2655 - 2664 (1997)

4. Dunning M.D., Kettunen M.I., Ffrench C.C., Franklin R.J.M., and Brindle K.M., "Magnetic resonance imaging of functional Schwann cell transplants labelled with magnetic microspheres," Neuroimage, 31 (1), 172 -180 (2006)

5. Kang C.H., and Kim W.G., "The effect of vasopressin on organ blood flow in an endotoxin-induced rabbit shock model," J. Investigative Surgery, 19 (6), 361 - 369 (2006)

6. http://www.mo-sci.com/Mo-Sci_Specialty_Products/Products/bond-line-Spacers/ (accessed - 12/11/06)

7. http://jazz.nist.gov/atpcf/prjbriefs/prjbrief.cfm?ProjectNumber=00-00-5424 (accessed - 01/13/07)

8. http://www.freepatentsonline.com/5177124.html (accessed - 02/06/07)

9. Rietema K. and Verver C.G., "Cyclone separators in Industry," Elsevier (1961)

10. Svarovsky L., "Hydrocyclones," Technomic Publishing Co., Inc. New York U.S. Patent No. 453, 105 (1984)

11. Seinfeld J.H. "Air pollution: Physical and chemical fundamentals," McGraw-Hill, Inc. USA (1975)

12. Cooper C.D. and Alley F.C., "Air pollution control: A design approach," Waveland Press Inc., IL, Second Edition (1994)

13. McCabe W., Smith J., Harriott P., "Unit operations of chemical engineering." McGraw-Hill, 6th edition (2001)

14. http://www.powerspan.com/technology/eco_overview.shtml#stage03 (accessed - 02/08/07)

15. Harper W., "Triboelectrification," Physical Education, 5(2), 87 - 93 (1970)

16. Yao K., "Design of high-rate settlers," J. Environ. Eng., 99, 621 - 637 (1973)

17. Richardson J.F. and Zaki W.N., "Sedimentation and fluidization," Trans. Inst. Chem. Eng., 32, 35 -53 (1954)

18. Rasul M.G., Rudolph V., and Wang F.Y., "Particle separation using fluidization techniques," Int. J. Miner. Process, 60, 163 -179 (2000)

19. Galvin K.P. and Nguyentranlam G., "Applications of reflux classifier on solid-liquid operations," Int. J. Miner. Process, 73, 83 -89 (2004)

20. Galvin K.P. and Nguyentranlam G., "Influence of parallel plates on liquid fluidized bed systems," Chem. Eng Sci, 57(7), 1231 -1234 (2002)

21. Laskovski, D, Duncan, P., Stevenson, P., Zhou, J., Galvin, K. "Segregation of hydraulically suspended particles in inclined channels," Chem. Eng Sci, 61, 7269 - 7278 (2006)

22. "Tilted-plate separator," Chemical Engineering, Jan 12, 60 (1970)

23. Davis, R., Zhang, X., and Agarwala J P, "Particle classification for dilute suspensions using an inclined settler," Ind. Eng. Chem. Res, 29, 1894 -1900 (1990)

24. Zhang, X. and Davis, R., "Particle classification using inclined settlers in series with underflow recycle," Ind. Eng. Chem. Res, 29, 1894 -1900 (1990)

25. Grbavcic Z., and Vukovic, "Single particle settling velocity through a liquid fluidized bed," Powder Tech., 66, 293 -295 (1991)

26. Davis R., Herbolzheimer E., Acrivos A., "Sedimentation of polydisperse suspensions in vessels having inclined walls," Int. J. Multiphas Flow, 8, 57 -585 (1982)

27. http://www.microtrac.com/laserdiffraction.cfm#theEquation (accessed - 03/05/07)

# VITA

Rajasekharan Pillai Annapoorneswari was born in Kerala, India on May 1, 1981. She received her primary education at St. Johns Public school in Kerala, India. In May 2002, she received her Bachelor of Technology in Chemical Engineering from University of Madras, Chennai, India. After which, she worked for almost two years in Strides Arco Lab Ltd, Mangalore, India as Research Engineer. She received her Master of Science in Chemical Engineering at the University of Missouri-Rolla in August 2007. She has been a Graduate Research Assistant in the Department of Chemical Engineering, University of Missouri-Rolla from January 2005 until May 2007. She was also a Graduate Teaching Assistant in the Department of Chemical Engineering, University of Missouri-Rolla from May 2005 until May 2007.